ANALYSIS, OPTIMIZATION, AND APPLICATIONS OF THE LIQUID PISTON HEAT ENGINE THROUGH DESIGN AND EMPIRICAL MODELING

A Thesis
Presented to
The Academic Faculty

By

Shawn Newlan

In Partial Fulfillment
Of the Requirements for the Degree
Masters of Science in Mechanical Engineering

Georgia Institute of Technology

August, 2017

ANALYSIS, OPTIMIZATION, AND APPLICATIONS OF THE LIQUID PISTON HEAT ENGINE THROUGH DESIGN AND EMPERICAL MODELING

Approved by:

Dr. Todd Sulchek, Advisor
Woodruff School of Mechanical Engineering
Georgia Institute of Technology

Dr. Cassandra Telenko
Woodruff School of Mechanical Engineering
Georgia Institute of Technology

Dr. Shannon Yee
Woodruff School of Mechanical Engineering
Georgia Institute of Technology

Date Approved: May 17, 2017

ACKNOWLEDGMENTS

I would like to thank Dr. Todd Sulchek for all his advice and help throughout my graduate career, for the encouragement of lifelong learning, and for developing a lab community that genuinely encourages scientific curiosity and intrigue. I would also like to thank Dr. Cassandra Telenko and Dr. Shannon Yee for their input and contribution to this work and for their previous research which has contributed toward this work.

Special thanks to the students and staff of Chattahoochee, Lassiter, and Kennesaw Mountain High School for their contributions towards developing technology which hopes to enlighten students on the concepts of thermodynamics.

TABLE OF CONTENT

ACKNOWLEDGMENTS iii

LIST OF TABLES vii

LIST OF FIGURES viii

LIST OF SYMBOLS x

SUMMARY xi

1. Introduction 1

1.1 Significance 1

1.2 Definitions 2

1.3 Working Principle 5

1.4 Background and Literature Review 8

1.4.1 Theory Based Research 11

1.4.2 Applications Based Research 13

2. Research Techniques 14

2.1 Engine Construction 14

2.2 Test Methods 16

2.3 Tips and Tricks 18

2.4 Limitations 19

3. Effects of Liquid Column Vaporization 21

3.1 Test Methods 21

3.2 Model Derivation 22

3.3 Experimental and Model Results 26

4. Engine Cycle Analysis 29

4.1 Apparatus 29

4.2 Results 31

4.3 Cycle analysis results 34

4.4 Vapor Contribution Analysis 36

4.5 Cycle Discussion 37

4.6 Chapter Discussion 40

5. Geometry Effects 41

5.1 Effects of height and length 41

5.2 Vapor Entrance Theory 43

5.3 Power Output Analysis 48

5.4 Parameter optimization 48

6. Novel Applications 50

6.1 Flexible and Bendable Waste Heat Powered Pumps 50

6.1.1 Engine Construction 51

6.1.2 Testing and Results 51

6.1.3 Flexible Pumping 53

6.1.4 Finite Element Analysis 54

6.2 Solar Powered Engines 57

6.2.1 Solar Engine Testing 57

6.2.2 Intensity Test Results 58

6.2.3 Engine Scalability 60

7. Educational Outreach 63

7.1 Thermodynamics Class Designette 63

7.2 High School Demonstrations 64

8. Conclusion 70

8.1 Intellectual Content 70

8.2 Future Directions 71

8.3 Conclusion 72

APPENDIX A: LIQUID VAPORIZATION TEST ENGINE 73

APPENDIX B: APPARATUS ENGINE 74

APPENDIX C: FLEXIBLE ENGINE 75

APPENDIX D: DEPTH SCALED ENGINE 76

APPENDIX E: CLASS QUESTIONNAIRE 77

REFERENCES 80

LIST OF TABLES

Table 1.1: Comparing the Wet and Dry Fluidyne 9

Table 3.1: Working liquids used during testing 21

Table 3.2: Working liquid mixtures 22

Table 3.3: Proportion of input energy toward vaporization and gas expansion 28

Table 4.1: Comparison of liquid piston and Stirling cycle 40

Table 5.1: Lengths and heights of engines tested 42

Table 5.2: Vapor entrance fitting parameters 46

Table 5.3: Engine height amplitude equation fitting parameters 47

Table 6.1: Thin flexible engine pumping results 54

LIST OF FIGURES

Figure 1.1: Engine components 3

Figure 1.2: Pumping configuration 4

Figure 1.3: Stirling engine operation 5

Figure 1.4: Schematic of conventional heat pipe 6

Figure 1.5: Engine oscillation 7

Figure 1.6: Variation in liquid piston engine designs 10

Figure 1.7: Non-Inertive-Feedback Thermofluidic Engine (NIFTE) 12

Figure 2.1: Steps for engine construction 14

Figure 2.2: Suspended heating element 15

Figure 2.3: Tracker video analysis software 18

Figure 3.1: Input power delivered to the working gas and liquid 22

Figure 3.2: Energy balance diagram 23

Figure 3.3: Performance analysis of different working fluids 26

Figure 3.4: Liquid vaporization experimental and model results 27

Figure 4.1: Cycle analysis engine 30

Figure 4.2 Block diagram of data collection process 31

Figure 4.3: Pressure, temperature, and volume profiles 32

Figure 4.4: Normalized pressure, volume, and temperature of cycles 33

Figure 4.5: Engine cycle PV diagram at 14.5 watts 34

Figure 4.6: Engine cycle analysis 35

Figure 4.7: Partial volume contributions to engine performance 37

Figure 4.8: Engine cycle discussion 37

Figure 4.9: TV diagram of engine cycle 38
Figure 4.10: Normalized temperature profile of engine thermocouples 39
Figure 5.1: Engine geometry with varying length and height 41
Figure 5.2: Performance results of varying lengths and heights 43
Figure 5.3: Vapor entrance at varying lengths 44
Figure 5.4: Effects of vapor entrance and viscous drag on amplitude 45
Figure 5.5: Height variation's impact on amplitude 47
Figure 5.6: Power output model with respect to length and height 48
Figure 6.1: The flexible liquid piston engine 50
Figure 6.2: Unbent unloaded performance of flexible engine 51
Figure 6.3: Bending characteristics of the flexible engine 52
Figure 6.4: Thick and thin engine performance with longitudinal bending 53
Figure 6.5: Flexible pumping configuration 54
Figure 6.6 FEA analysis of flexible engine 55
Figure 6.7: Solar Engine 57
Figure 6.8: Radiation shield 58
Figure 6.9: Intensity test apparatus 59
Figure 6.10: Radiative intensity's effect on solar engine performance 59
Figure 6.11: Solar engine scalability 61
Figure 7.1: Pre & post-test results from thermodynamics designette 64
Figure 7.2: Students actively learning 66
Figure 7.3: Sample questions from manual 68
Figure 7.4: Arbor Scientific thermodynamic lab kits 69

LIST OF SYMBOLS

Carnot efficiency	η_{carnot}
Beale Number	$B_n = 0.0147$
Stroke volume	V
Peak-to-peak amplitude of oscillation	S
Output power	$\dot{W}_{out}$
Gravitational acceleration	$g = 9.81\ m/s^2$
Liquid density	ρ
Enthalpy of vaporization	ΔH_{vap}
Specific volume of gas	v_g
Frequency of oscillation	f
Pressure	P
Temperature of hot reservoir	T_H
Temperature of cold reservoir	T_C
Hydraulic head	h_f
Darcy-Weisbach friction factor	f_D

SUMMARY

The liquid piston heat engine demonstrates a unique thermofluidic phenomenon of steady state volumetric oscillation. This engine, which has no moving parts, operates at low temperature differentials, and has unmet potential in the fields of waste heat collection and water distribution. A range of research was performed to better understand the liquid piston heat engine's operation and potential applications. The research performed and discussed in this thesis has led to the creation of flexible, dual chamber engine [1] and small solar engines. This work presents a better understanding of the engine's thermodynamic cycle and the effects that fluid vaporization and engine geometry have on engine performance.

Along with the research performed to better understand the engines, additional work has been performed to demonstrate the potential for using the simple engine as an educational apparatus. This thesis describes how the engine can be used to help undergraduates and high school students gain a better understanding of thermodynamics through quantitative analysis of engine operation.

Due to the engine's current inefficiencies, the simple and robust machine has yet to reach its full potential. However, it is the contribution of this thesis to increase the body of knowledge of the thermofluidic mechanisms underpinning the engine operation with the hope that their applications may one day benefit our society.

1. Introduction

1.1 Significance

Energy lost to waste heat is a ubiquitous part of modern life. The US alone consumes nearly 100 quadrillion BTUs a year [2] much of which is ultimately lost in the form of waste heat. In the US 60% of waste heat is left unrecovered [3] due primarily to the high cost of infrastructure associated with capturing the energy. The vast majority of waste heat conversion is in the form of heat transfer through heat exchangers. Capturing low quality heat (<150°C) for useful work is particularly ignored due to the low efficiencies of systems which may capture and utilize the heat. One method in reducing such waste is to make more efficient heat collection systems such as those that run on the organic Rankine cycle (ORC)[4]. However, even the most efficient of systems will leave much of the low-quality energy unrecovered due to the Carnot limit (1), in which the engine efficiency is limited by the temperatures of the hot and cold reservoirs.

$$\eta_{carnot} = 1 - \left(\frac{T_C}{T_H}\right) \tag{1.1}$$

An alternative approach to low quality heat conversion is to focus not on improving efficiency, but reducing the cost of system implementation [5]. Though the efficiency of any system will be limited, waste heat is abundant and largely unutilized. Therefore, by considering a system cost per power output metric ($/watt) [6], even low efficiency engines may have useful applications provided the useful work exceeds total operation costs. Regarding low cost manufacturing and operation of heat engines, the liquid piston heat engine offers unique potential. The engine is composed simply of a working fluid and a working gas retained in a certain geometry by inexpensive and easily manufactured

materials. Because the working fluid can be water and the working gas air, the low cost of construction and available materials offers a great deal of potential in certain niche applications [5].

Though manufacturing costs are incredibly low, the potential for such a simple energy conversion device has yet to be fully achieved. These engines, which naturally lend themselves to pumping applications, could become an important part of active heat transfer and water management techniques, particularly in regions where maintenance and available materials are limited [7].

Along with the direct value of transferring energy, the simple engines also offer value in an indirect way: the transfer of knowledge. Many students find the subject of thermodynamics counterintuitive and experience difficulties grasping some of the core concepts which modern thermodynamic systems are built [8]. There exists a need to provide simple demonstrations of thermodynamics so that student may better understanding working principles. Lab kits do exist that demonstrate thermodynamics, however they are typically too complicated to be practical tools used in classrooms for students being exposed to the material for the first time [9]. Additionally, the design of the liquid piston engine lends itself to simple data collection and quantitative analysis. By applying these engines to designettes and in-class lab exercises a useful tool can be created for developing a student's understanding of thermodynamics [8][10][11].

1.2 Definitions

For consistency, the following terms will be used throughout this thesis when referring to the components of the engine.

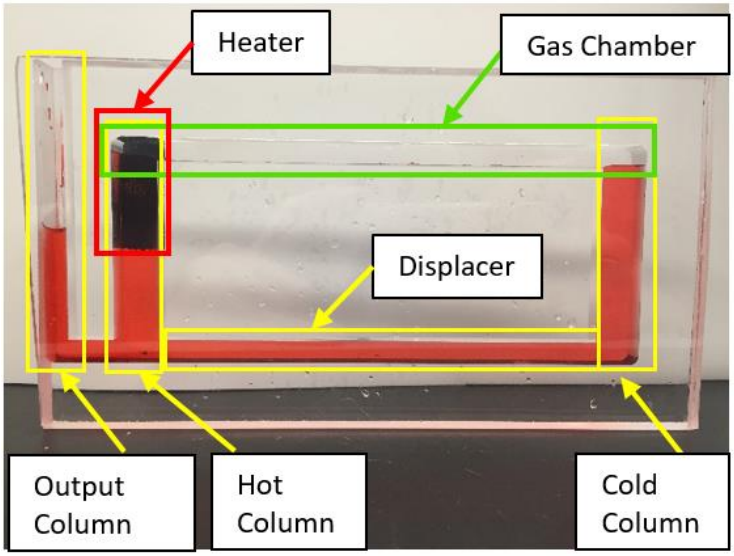

Figure 1.1: Engine components

- **Heater:** Source of input energy
- **Hot column:** The liquid column which contains the heater
- **Cold column:** The liquid column not exposed to the heater
- **Output column:** The liquid column exposed to ambient pressure. This column is where fluid oscillation is recorded
- **Gas chamber:** The gas-phase portion of the engine which contains the working gas and vapor
- **Displacer:** The liquid chamber of the engine which connects the hot and cold columns
- **Working liquid:** The liquid-phase working fluid which composes the liquid columns and displacer
- **Working vapor:** The vaporized component of the working liquid
- **Working gas:** The non-condensable gas contained in the gas chamber. Throughout this research air was used as the working gas and is assumed to be ideal

We propose that the engine converts heat to produce work through exploiting volumetric oscillation of the gas chamber. The oscillation is due to mass fluctuation of the working

vapor, as well as the expansion and compression properties of the working gas. The volumetric oscillation of the gas chamber can be observed by the vertical displacement of the output column due to the assumed incompressibility of the working liquid.

When the output column is exposed to ambient pressure, it is said to be in an **unloaded configuration** [12]. Because all work done by the engine onto the environment is returned to the engine during its compression stroke (excluding viscous losses), the engine is said to be in a net zero power output arrangement. When the engine is connected in a check valve arrangement (Figure 1.2) it is said to be in a **loaded configuration** in which useful power output is obtained through pumping.

.

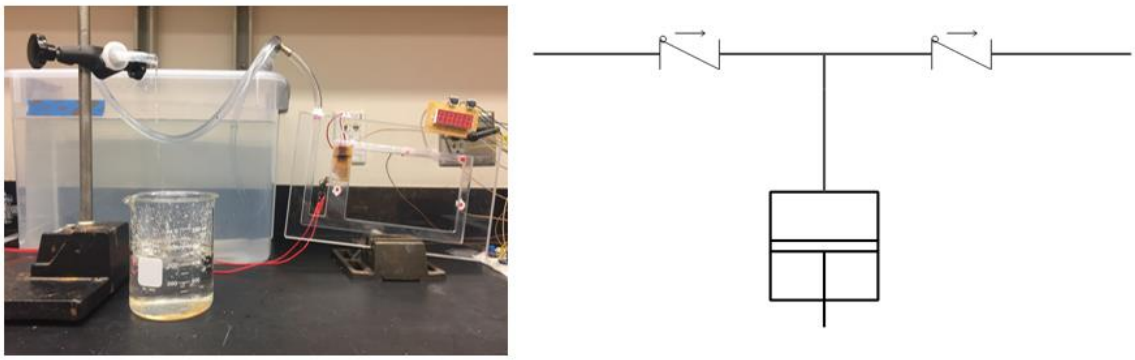

Figure 1.2: Pumping configuration
(A) Engine in loaded configuration (B) Hydraulic diagram of pump

Pumping is achieved by pulling liquid into the system through the inlet check valve during the compression stroke and pushing liquid out of the system through outlet check valve during the expansion stroke. In congruence with check valves, the volumetric oscillation of the engine's gas chamber creates a *liquid piston reciprocating positive displacement pump*. Because these engines typically run with water as the working liquid and air as the

working gas their potential for waste heat harvesting lend themselves to this pumping applications [12][5].

1.3 Working Principle

To understand the operation of the liquid piston heat engine it is important to also understand the functionality of both Stirling engines and heat pipes.

Stirling Engines

Stirling engines operate off the expansion and compression of an enclosed working gas. The gas is shuttled, via piston, between hot and cold sources where it transitions between isothermal expansion or compression (1 and 3) and isochoric cooling or heating (2 and 4) states to produce an engine cycle (Fig. 1.3.A).

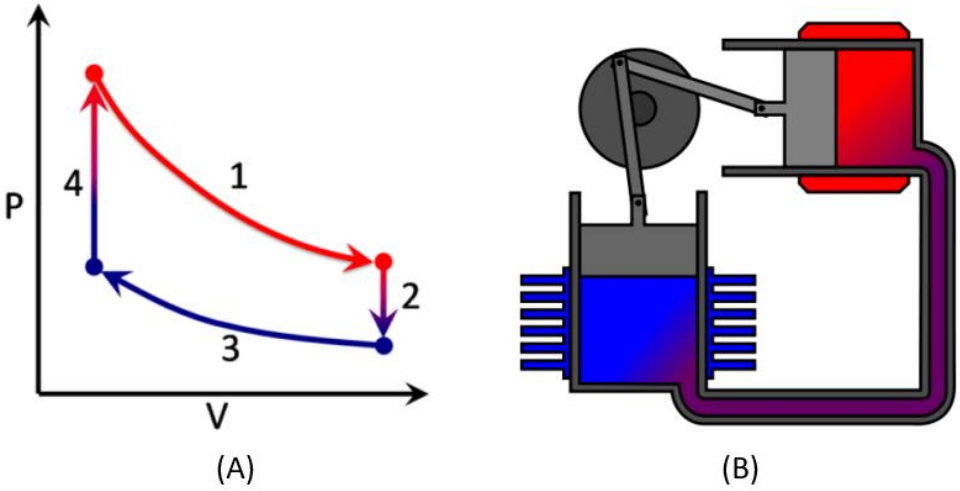

Figure 1.3: Stirling engine operation
A) Stirling engine cycle (B) Alpha Type Stirling Engine [13]

The benefit of Stirling engines is that the enclosed working gas does not require combustion or exhaust and may effectively run off temperature differential alone. Though Stirling engines can be efficient heat engines, they require mechanical mechanisms, and costly and complex piston seals to operate effectively [12][13][7].

Heat Pipes

Heat pipes are effective rigid cooling devices which can transfer energy away from a hot source to a cold sink more quickly than what can be achieved from conduction alone. Heat pipes operate on the principle of transferring latent heat due to phase change of a working fluid.

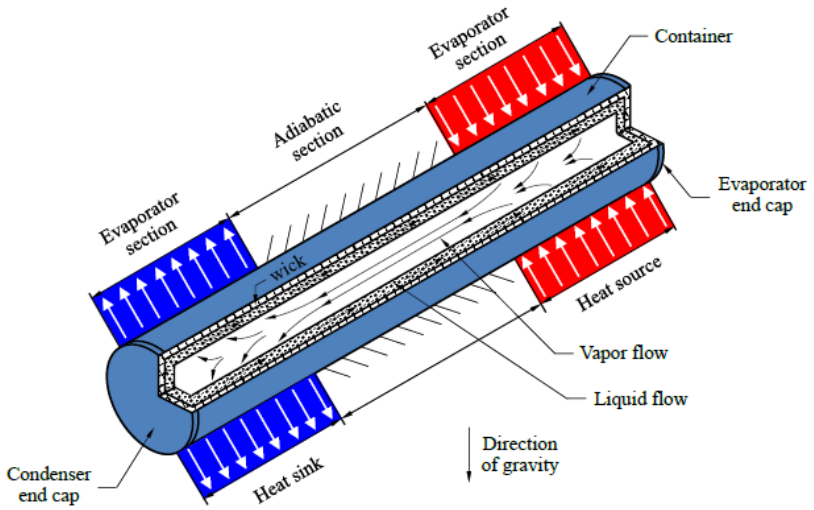

Figure 1.4: Schematic of conventional heat pipe
[14]

At the hot end of the pipe (evaporator section) the working fluid will vaporize and absorb energy. The vapor then travels (typically in the center) through the pipe to the cold end (condenser) where the fluid condenses and releases energy. The condensed liquid then travels back to the hot end via capillary forces and the cycle continues [14].

Liquid Piston Heat Engines

The liquid piston engines tested in this research have a similar operation to heat pipes in that a two-phase working fluid is vaporized at the hot end and condensed at the cold end, creating a circular mass flow of vapor and liquid along the length of the gas

chamber and the liquid columns/displacer, respectively. Mass flow and transfer of latent heat alone will not create the volumetric oscillation needed for pumping.

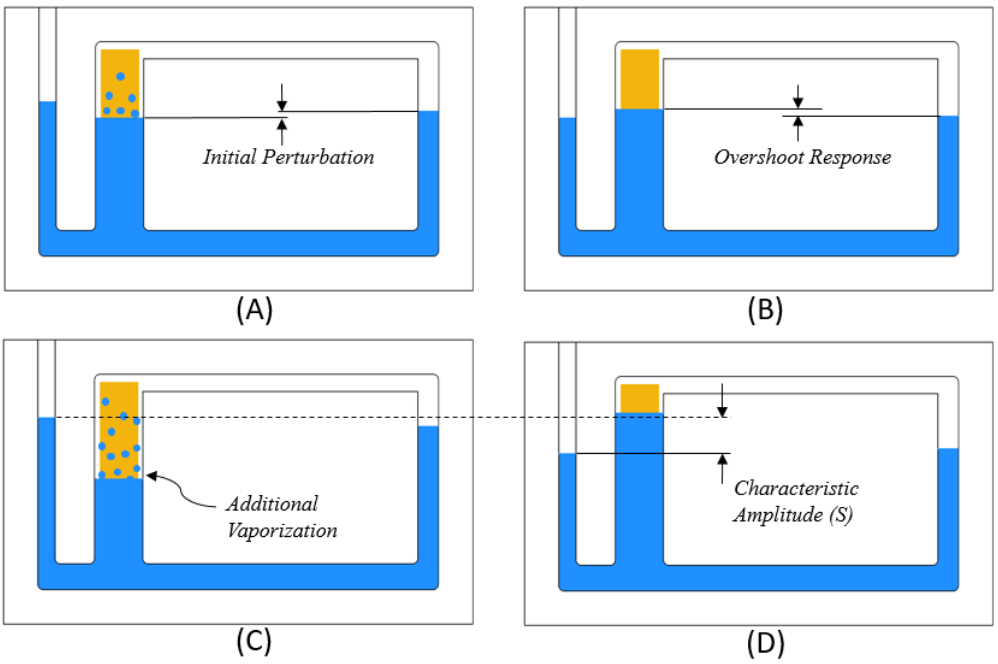

Figure 1.5: Engine oscillation
(A) Initial perturbation (B) Equilibrium overshoot (C) Periodic liquid in cold column (D) Periodic liquid in hot column

We conjecture that oscillation begins due to a perturbation created by the vaporization (specifically boiling) of the working liquid in the hot column. The boiling creates a small, erratic, pressure differential between the hot and cold column surfaces. This small pressure differential puts the "U" formation of the liquid channel into an unstable state (Figure 1.5A). When liquid oscillates back into the hot column, to equalize the pressure, it will slightly overshoot the initial equilibrium, thus more liquid is exposed to the hot column and additional vaporization occurs (Figure 1.5B). When calibrated correctly, the initial perturbation creates a positive feedback loop in which the working liquid will begin oscillating back and forth between the hot and cold columns at a characteristic frequency

and amplitude (Figure 1.5C and D). With this periodic oscillation of the working liquid, there is also a periodic variation in the vapor mass flow, and thus volume, within the gas-phase chamber. It is with this volumetric variation that useful work can be derived from the system.

Along with creating periodic change in mass flow, the oscillation of the working fluid also shuttles a working gas between the hot and cold columns. It is with shuttling of the working gas that the working liquid acts as pistons for the engine putting the gas into an approximate Stirling cycle. For large engines, the Stirling cycle is a critical factor for engine operation and liquid vaporization is actively avoided to improve efficiency [12]. However, with smaller engines it is in question the significance that the Stirling cycle has on engine performance as compared to the variation in vapor mass flow created by the oscillating columns. This question is explored in more depth in chapters 3 and 4.

1.4 Background and Literature Review

Though the concept of liquid piston engines is nothing new, with patents dating back as far as the 1600s [12], they still remain a relatively unexplored subject in modern engineering. The Fluidyne engine, which in different forms can be referred to as a thermofluidic oscillator, thermoacoustic heat engine, free piston engine, liquid piston Stirling engine, or simply liquid piston heat engine, was primarily researched in the 1970s-1990s [12][15][16]. By far the most significant work regarding Fluidyne engines is the book: *The Liquid Piston Stirling Engine* by C.D West. Dr. West and his group at Oak Ridge National Labs (ORNL) were pioneers in the research, collaboration, and distribution of information regarding liquid piston engines with primary application for large scale water pumps. *The Liquid Piston Stirling Engine* provides a concise general review of liquid

piston engine research as well as provides design suggestions and direction for future research regarding large scale pumping. Though concise and thoroughly researched in the context of large scale liquid pistons, there were still many unknowns about the engine's operation at the time of the books inception.

Fluidyne engines can be broken up into two primary categories: *Dry* and *Wet* [12].

Table 1.1: Comparing the Wet and Dry Fluidyne

Wet Fluidyne	Dry Fluidyne
Powered by vapor cycle	Powered by Stirling cycle
Low Efficiency: <1%	Higher Efficiency: >10%
High Power Density	Low Power density
Small, Simple	Large, More Complex
Low temp. differential	High temp. differential

Dry Fluidynes, which are the primary topic of West's book, operate on the Stirling cycle by shuttling a working gas to and fro between the hot/cold columns. Dry Fluidynes do not require the additional pressure differentials created by piston vaporization and are, in contrast, designed to limit vaporization (through use of seals, and low-volatility liquids) to improve efficiency. Because dry Fluidynes have significantly lower power densities than wet Fluidynes they tend to be larger and operate at higher temperature differentials to overcome internal viscous forces of the liquid pistons. Wet Fluidynes, as the inverse, require vaporization to create oscillation in the system. The significant effects that vaporization and condensation have on gas chamber volume allows for the engines to be small and operate at low temperatures while still being able to overcome viscous losses of relatively narrow channels. The draw back with vaporization/condensation is a significant amount of energy, thus efficiency, is lost due to transfer a latent heat [17].

Along with being wet and dry, liquid piston engines come in many different arrangements. These engines range from the simplest formation of the alpha-type Fluidyne (Figure 1.6.A) to highly complex systems for modern research. A commonality that nearly all these engines share is the connection of the liquid columns between the hot and cold reservoirs, and the use of liquid as piston drivers to create volumetric oscillation.

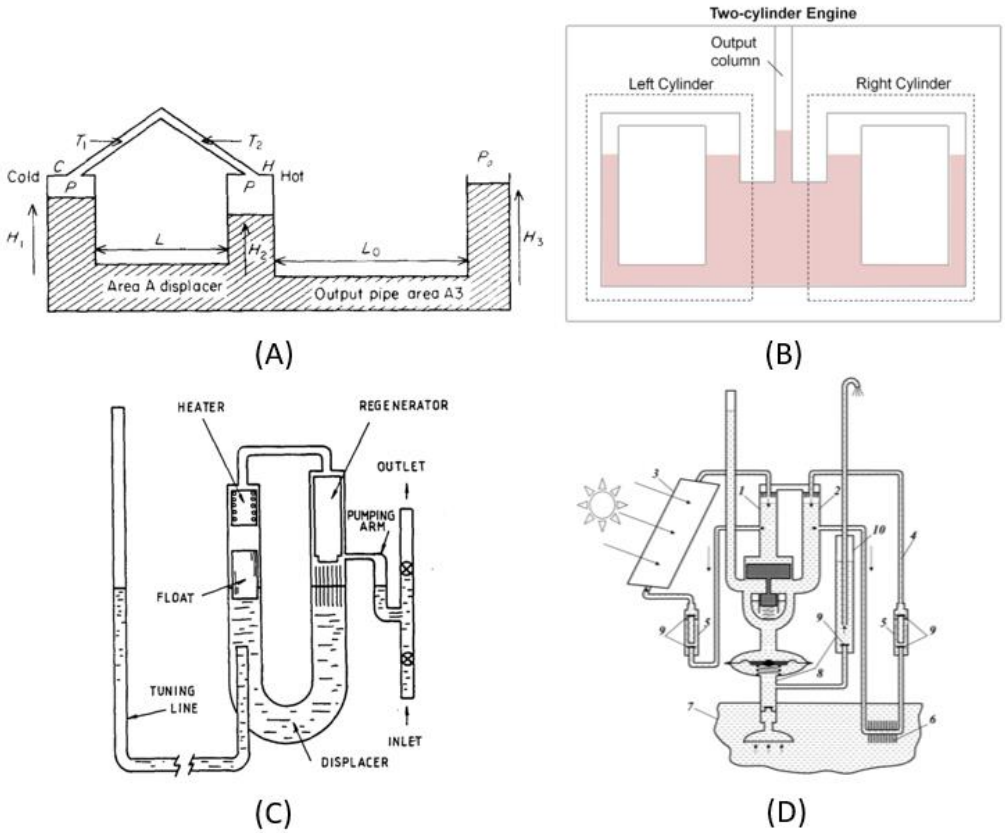

Figure 1.6: Variation in liquid piston engine designs
(A) Alpha-Type Fluidyne [18] **(B) Two-Cylinder Liquid Piston Engine [1]**
(C) Liquid Feedback Fluidyne [19] **(D) Solar Thermal Water Pump** [7]

Research on liquid piston engines has recently been focused into the categories of theoretical and applications oriented research.

1.4.1 Theory Based Research

Much of the recent theory driven research around liquid piston engines is the attempt to mathematically model and predict their behavior. Though the early researchers Stammers, Reader, and West all derive equations to predict the behavior of the two-phase engine they remain inconclusive, particularly for the loaded configuration. The culmination of fluid inertia, viscous losses, vapor-gas partial pressures, and pressure fluctuations due to phase change all within a dynamically oscillating system has presented a starkly complex problem in a very small package. Within the last decade, the two major groups which have contributed to mathematically modeling this dynamic system are Özdemir, Arslantürk, and Özüç out of Istanbul and Markides and Smith out of London.

The Turkish group has published several papers to derive a mathematical understanding of the engine. The group was able to derive a model which produced good agreement with experimental values, however this model works only with engines in a net-zero power output scenario (unloaded configuration) as is made clear by their statement:

> "it is clear that the mechanism and the mathematical model of the interfacial evaporation and condensation phenomena on the oscillating liquid columns are weaknesses of this study" [20].

The London group focused their contribution to examining the 'Non-Inertive-Feedback Thermofluidic Engine' (NIFTE) [15]. An important aspect of the geometry of the output column and displacer is the mass of the liquid acting as an inertial element in the dynamic system. Because the inertial element is less influential while the engine is in a loaded configuration, the group attempted to develop a model for this non-inertive

system. For the NIFTE system (Figure 1.7A) the group developed a mechanical-electrical analogy circuit (Figure 1.7B) to model the engine's behavior.

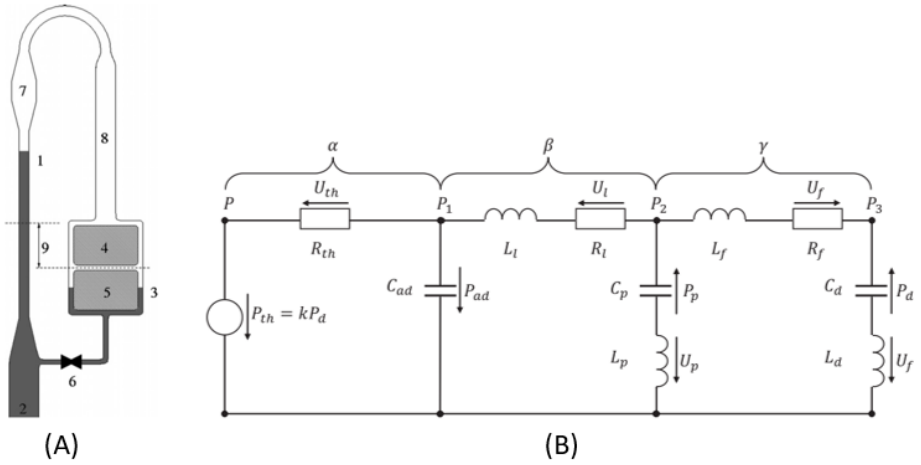

Figure 1.7: Non-Inertive-Feedback Thermofluidic Engine (NIFTE) (A) NIFTE system (B) Mechanical-electrical analogy circuit [15]

Though rigorous in complexity the group ultimately found that inertive effects of the fluid oscillation cannot be ignored even in the loaded configuration:

> "Further, the predictions from the non-inertive model diverge significantly from experimental observations. We conclude that inertia may constitute an important factor in the modelling of this system" [15].

The researchers mention that inertia may be an important factor on the feedback valve's drag on marginal gains. Though still inconclusive with mathematical modeling, Markide's group continues to study the potential of two-phase thermofluidic engines for collecting waste heat. Their current research uses a more mechanical system than the NIFTE and is geared towards application, but the machine is still largely driven by Fluidyne principles [3].

It is clear that more work is needed to produce predictive models which may optimize these hydrodynamic systems.

1.4.2 Applications Based Research

There have been several recent systems developed to explore the potential of these engines for waste heat collection. A notable early successful example of this engine's application was built by Metal Box Co. of India which claimed their Fluidyne pump could achieve a theoretical output of 4.3 L/s [21]. This early adapter was successful in demonstrating the useful potential in liquid piston technology. Within the last decade, four separate groups have demonstrated successful application of novel uses for pumping. Steven's group uses a Fresnel lens to focus sunlight to deliver energy to an alpha-type engine's hot column [22], which he uses to characterize the internal cycle. Orda used solar collecting heater plates to deliver energy into a relatively complex Fluidyne and was successful in producing pumping up to 0.7 m^3/hr. Orda suggested the design could be useful in circulating water for the fish-agro industry [7]. Van de Ven suggests that a liquid piston system can be used for a mobile hydraulic power supply that may run off thermal batteries such a liquid salt as opposed to electricity [23]. Finally, Slavin uses a Fluidyne system as a medium to convert heat to electricity by pumping water through a turbine [24].

In all cases, the systems were proof of concept that the liquid piston engine has merit for modern uses. There is still much unknown about the operation of the two-phase engine, particularly in how to optimize its operation while in a loaded configuration, but it is the goal of research such as this to contribute to a greater understanding of this mechanism.

2. Research Techniques

2.1 Engine Construction

For the majority of this research, the engines tested were created by milling engine geometries into 1/2” clear acrylic panels. Once the panels were milled, Kapton resistive heating elements were added to the hot column. After adhering the heater within the milled engine geometry, the engines are then sealed with a second 1/8” clear acrylic panel which is chemically bonded to the engine block through the use of acrylic cement.

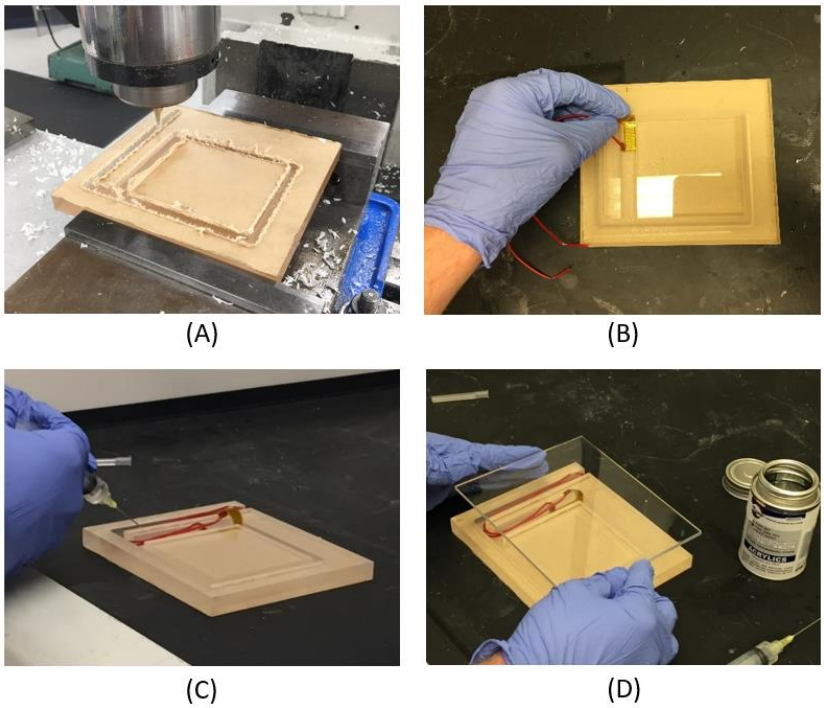

Figure 2.1: Steps for engine construction
(A) Engine block being milled. (B) Adhesion of heating element. (C) Applying acrylic cement via syringe (C) Sealing of the engine with a cover panel

Acrylic was chosen as a material for testing the engines as it is a widely accessible, transparent, and pliable material with a suitable working temperature for the ranges tested [12]. Note that with some engines the acrylic did experience damage (cracking and melting) at the location of the heater (Figure 2.2.A). This can be avoided by suspending

the heater within the engine's hot column so that none of the element makes direct contact with the acrylic engine surface (Figure 2.2.B). This suspended heater method provides the added benefit of more fully transferring heat to the working gas and liquid column.

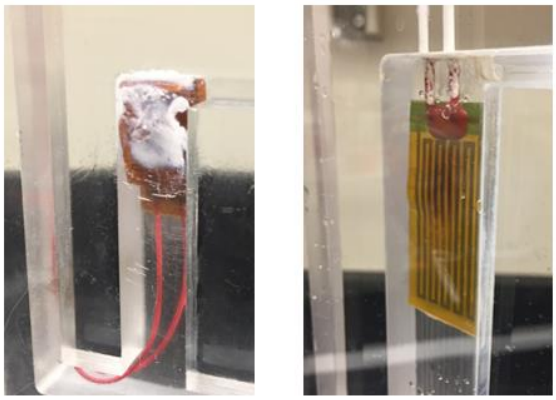

Figure 2.2: Suspended heating element
(A) Engine damage due to adhered heater (B) Isolated heater suspended in the hot column

Though engines designed to collect waste heat would not have a heater, but rather conductive material contacting a hot reservoir, the heating elements allow for accurate monitoring of input power during testing.

In addition to the standard acrylic engines, more complex methods and geometries were also explored and will be discussed in further depth in Chapter 6. Note that with all engines created in this research the columns are made at right angles. Though sharp angles do add to internal losses [25], this was an intentional decision to be consistent with research performed previously within the Sulchek group. Additionally, the geometry allows for the isolation of the effects of height and length when testing engine geometry parameters. These engine geometry parameters are explored in more depth in Chapter 5.

2.2 Test Methods

For many sections of this thesis describing the research, the engines have been tested in an unloaded configuration, meaning that the oscillation in the output column is exposed to ambient pressure. Because all work done by the engine to the environment is returned to the engine during its compression stroke, the engines are typically tested in a net zero power output arrangement. It is however, an understanding that high frequency and large amplitude of liquid oscillation for an engine represents a large potential power output. In order to understand the potential power output created by this type of engine, equation 2.1 is applied for the unloaded engine to estimate the potential power output [12][11][26].

$$\dot{W}_{out} = B_n P V f \tag{2.1}$$

Where $\dot{W}_{out}$ is the potential power output, V is the stroke volume of the output column, P the average operating pressure of the engine (assumed to be atmospheric), and f the frequency of oscillation. The Beale number B_n is an empirically derived figure widely used to make estimates of the performance of new designs and compare the performance of existing engines [12], [26]. The Beale number may range from 0.15 to 0.11 for engines with high temperature differentials, and may also be as low as 0.005 for very small temperature differentials (closer to the range which these engines were tested). To calculate the Beale Number used in this thesis an engine was tested in both an unloaded and loaded configuration at the same input power (14.6 W). Power derived from the *loaded* configuration was calculated using equation 2.2.

$$\dot{W}_{out,loaded} = \rho g h V f \tag{2.2}$$

Where stroke volume is the measured output of water per cycle. The hydraulic head $\boldsymbol{h}$ is equal to the sum of the height difference between the outlet valve and inlet water level plus the head differential created by the check valves (measured to be 13 cm). This measured output power was then compared to the unloaded performance of the engine operating with the same input power. Thus, equation 2.3 was used to derive our Beale Number using the stroke volume and frequency of the unloaded configuration.

(2.3)

$$\boldsymbol{B_n = \frac{\dot{W}_{out,loaded}}{PVf}}$$

Through testing our engines achieved a Beale Number as high as 0.0147 which will thus be set as the value for calculations throughout this thesis. Note that a Beale Number of 0.0147 is higher than the upper limit originally approximated by West for our temperature rang $B_n(T = 100°C) < 0.010$ [26]. However, our lab has consistently achieved higher values.

To accurately record engine stoke volume (oscillation) and frequency, which are necessary for the potential power (equation 2.1), open source video analysis software Tracker was used [27]. Before recording a ruler is fixed next to the output column to accurately determine amplitude of oscillation. After steady state oscillation is achieved a video is recorded to accurately determine cycle amplitude and frequency (typically 30 seconds to 1 minute), the video is then uploaded to tracker software. Tracker software has an "Auto Track" functionality which may automatically follow an object within the video relative to an XY plane.

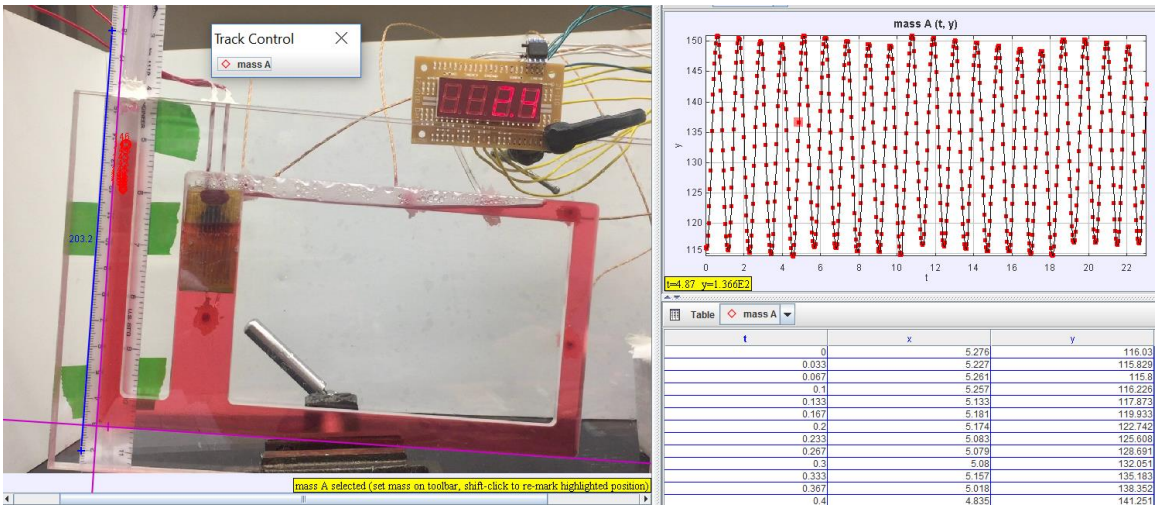

Figure 2.3: Tracker video analysis software

Note: The autotracker functionality is susceptible to drift and requires strong contrast to work affectively. Dye is typically added to the working liquid to increase video contrast. Object points may also be tracked manually which allows for correction of bias within the software. The point locations (chosen at the meniscus of the desired column) and their respective time stamps can be exported to excel or MATLAB for data analysis. This method is used for all experiments which involve frequency and stroke volume analysis.

A power supply is used to deliver energy to the resistive heating elements. Typical input power ranges from 3-8 W and does not exceed 28 volts. In order to gather pumping results from the engines a check valve arrangement is used as discussed previously in Section 1.2. Additional testing methods were used on case by case basis and are discussed when applicable.

2.3 Tips and Tricks

As with all research, after performing many experiments with a certain system, general difficulties arise and must be overcome. Working with the wet Fluidynes can be frustrating at times, particularly with smaller scale engines, because of their low power

output. The following are some general qualitative understandings from experience to obtain desirable performance with the engines. There is a vast amount still unknown about these engines thus this sections aims to help future researchers who would like to explore similar work.

1. Be patient – The engines take some time to start up, particularly large ones. Typically, larger engines take 20 min before reaching steady state amplitude.
2. Initial gas volume is important – The engines will not operate without some portion of the gas chamber being composed of a working gas.
3. Slowly heating the engine can help prevent "over heating" the engine. If the engine is heated too rapidly the gas volume will expand to a point where the liquid column no longer contacts the heater effectively turning off the engine.
4. The initial height of fluid in the output column contributes to how smoothly the engines may oscillate. The liquid column works as an inertial element helps provide stability to the system and helps prevent erratic oscillation due to vaporization at the hot column.
5. Tilting the engines is effective technique in increasing the total power output of the engine.
6. Acrylic is an easily accessible material for this research but also has its limitations, namely melting for higher temperatures. Consider alternative materials, such as Kapton, which are more resistant to high temperatures.

2.4 Limitations

The largest limitation in dealing with these engines is balancing out the natural resonances within the system. Geometry, initial gas and liquid volume, input energy, and

engine tilt angle all effect the performance of the engines in a way that may be unpredictable. Finding a balance for these resonances often leads to engine designs with less than desirable performance, though most will still work to some degree. Very little literature exists about liquid piston heat engines and even less is known on the operation of wet Fluidynes.

Though practical application of the engines is currently limited, quite possibly the most important knowledge that can be achieved from wet Fluidynes is to understand how power can be derived from the mass transfer of a two-phase fluid. Because of the educational focus, availability of materials, and the precedent of previous research performed within the Sulchek group, the whole of this research focuses on the ***alpha-type wet Fluidyne***.

3. Effects of Liquid Column Vaporization

To better understand the contributions that vaporization of the liquid pistons has on engine performance, a variety of working liquids were tested. These liquids varied in heat of vaporization so that the effects of vaporization could be isolated. A model, based on conservation of energy, was developed to predict the behavior of these engines with different working liquids.

3.1 Test Methods

For the liquid vaporization experiments 4 liquids were used. Water, Isopropyl Alcohol (91% IPA), Ethylene Glycol, and Methanol (99.8%). These liquids were used due to their varying heat of vaporization properties.

Table 3.1: Working liquids used during testing

Liquid	Heat of Vaporization (kJ/mol)	Vapor Pressure @100°C (Pa)
Methanol	37.00	373302
Isopropyl Alcohol (91%)	39.88	202649
Water	40.66	87726
Ethylene Glycol	65.60	2466

Along with being tested independently, mixtures of the liquids were created to achieve a greater variation of vapor pressure to understand how fluid vaporization is related to engine performance. The fluids were mixed volumetrically and vapor pressure was calculated through Raoult's Law using molecular fractions [28].

Table 3.2: Working liquid mixtures

Mixture	Ratio (vol. - vol.)	Vapor Pressure @100°C (Pa)
Glycol, Water	25 – 75	82004
Glycol, Water	50 – 50	72592
Glycol	100	2466
Water	100	87726
IPA, Water	22.75 – 77.25	92803
IPA, Water	45.5 – 54.5	101039
IPA, Water	74.25 – 25.75	123530
IPA, Water	91 – 9	158223
Methanol, Water	25 – 75	113422
Methanol, Water	50 – 50	153057
Methanol, Water	75 – 25	222194
Methanol	100	373302

The engines used for this experiment were of the primary type used throughout this research (1/2” milled Acrylic with a Kapton sealed resistive heating element). Dimensions of the engine used in these experiments may be found in appendix (A). The engines were tested using two methods: Variation of input power for the 4 base chemicals, and variation of chemical mixtures at a constant input power (4.8 W).

3.2 Model Derivation

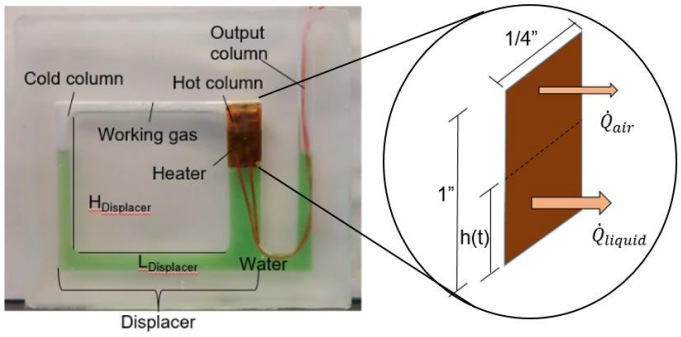

Figure 3.1: Input power delivered to the working gas and liquid

The model for the engine performance which accounts for enthalpy of vaporization is developed through conservation of energy. In this thermodynamic system, the input

power is the heat energy delivered from the heating plate. The value of $\dot{\boldsymbol{Q}}_{\boldsymbol{in}}$ is assumed to be equal to the resistive heating power calculated from current and voltage set in the DC power supply.

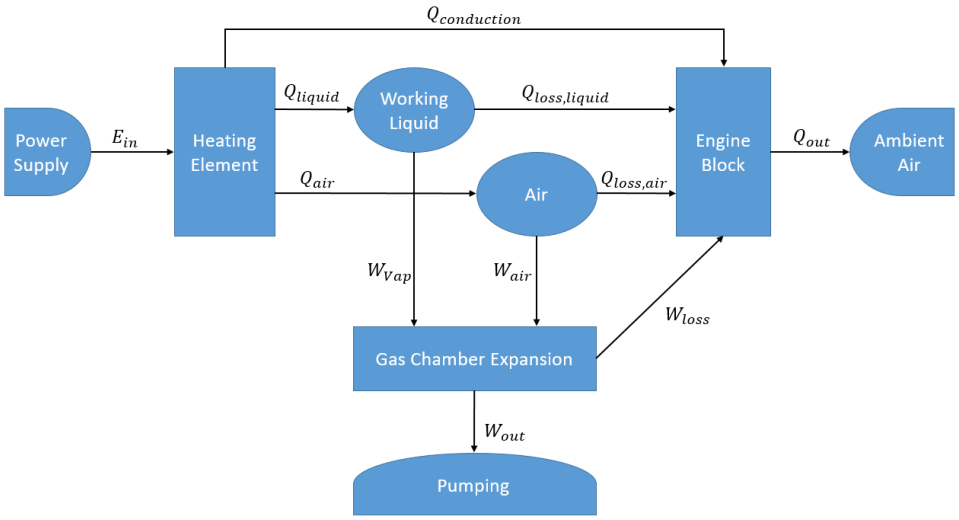

Figure 3.2: Energy balance diagram

The heating plate heats both the air and liquid column through convection as well as the engine block directly through conduction. Thus, the input power ($\dot{\boldsymbol{Q}}_{\boldsymbol{in}}$) can be divided to $\dot{\boldsymbol{Q}}_{\boldsymbol{air}}$, $\dot{\boldsymbol{Q}}_{\boldsymbol{liquid}}$ and $\dot{\boldsymbol{Q}}_{\boldsymbol{condution}}$.

$$\dot{\boldsymbol{W}}_{\boldsymbol{out}} = \underbrace{\dot{\boldsymbol{Q}}_{\boldsymbol{liquid}} + \dot{\boldsymbol{Q}}_{\boldsymbol{air}} + \dot{\boldsymbol{Q}}_{\boldsymbol{condution}}}_{\dot{\boldsymbol{Q}}_{\boldsymbol{in}}} - \dot{\boldsymbol{Q}}_{\boldsymbol{out}} \tag{3.1}$$

It is understood that useful work is created by volumetric change in the gas chamber. Thus, useful work is created by gas expansion and liquid vaporization. By separating the input energies to both the air and liquid (Q_{air}, Q_{liquid}) into terms of work delivered (W_{air}, W_{vap}) and heat lost ($Q_{a,loss}, Q_{l,loss}$) we my isolated the desired work terms. The total heat removed from the system (Q_{out}) is composed of the heat transferred to the engine

block through: conduction from the heater ($Q_{conduction}$), convection from the working liquid and gas ($Q_{a,loss}, Q_{l,loss}$) , and frictional losses from the fluid motion ($\boldsymbol{W_{loss}}$).

$$Q_{liquid} = Q_{l,loss} + W_{vap} \quad , \quad Q_{air} = Q_{a,loss} + W_{air}$$

$$Q_{out} = Q_{conduction} + Q_{loss,air} + Q_{loss,liquid} + \boldsymbol{W_{loss}}$$

Thus work terms may be isolated in the form:

$$\boldsymbol{\dot{W}_{out} = \dot{W}_{air} + \dot{W}_{vap} - \dot{W}_{loss}} \tag{3.2}$$

Since the engines were tested in an unloaded configuration, i.e. pumping not being performed, potential power is calculated through equation 2.1 utilizing the Beale Number ($\boldsymbol{B_n}$). Output power ($\boldsymbol{\dot{W}_{out}}$) is calculated using the Beale number, in combination with the stroke volume (V), working pressure ($\boldsymbol{P}$), and frequency ($\boldsymbol{f}$). Note that stroke volume is the product of peak-to-peak oscillation amplitude ($\boldsymbol{S}$) and the area of the output column ($\boldsymbol{A}$) [12][11][26].

$$\boldsymbol{V = SA} \quad , \quad \boldsymbol{\dot{W}_{out} = B_n VPf}$$

$$\boldsymbol{\dot{W}_{out} = B_n SAPf} \tag{3.3}$$

To determine the contribution of vaporization to stroke volume, we assume the pressure changes negligibly, i.e. the cyclical internal pressure change (ΔP) of the engine is much less than that of the engine's operating pressure (P_{atm}).

$$P_{atm} \gg \Delta P \quad \therefore \quad P \approx Constant$$

With this assumption, the work done through vaporization ($\boldsymbol{W_{vap}}$) may be calculated by the product of pressure and vapor volume change. Where vapor volume change is defined by the energy absorbed in vaporization ($\boldsymbol{Q_{vap}}$) multiplied by the specific volume of the

vapor ($\boldsymbol{v_g}$) at the hot column temperature (assumed to be 100°C) over the heat of vaporization ($\Delta \boldsymbol{H_{vap}}$). Thus, we establish an inverse relationship between heat of vaporization and work generated due to vaporization in equation (3.4).

(3.4)

$$\boldsymbol{W_{vap}} = \int PdV = P\Delta V = \boldsymbol{P}\left(\frac{\boldsymbol{v_g}}{\Delta \boldsymbol{H_{vap}}}\right)\boldsymbol{Q_{vap}}$$

By combing equations 3.2, 3.3, and 3.4 a fully developed model of driving variables is shown.

(3.5)

$$\boldsymbol{B_n SAPf} = \boldsymbol{P}\left(\frac{\boldsymbol{v_g}}{\Delta \boldsymbol{H_{vap}}}\right)\dot{\boldsymbol{Q}}_{\boldsymbol{vap}} + \dot{\boldsymbol{W}}_{\boldsymbol{gas}} - \dot{\boldsymbol{W}}_{\boldsymbol{loss}}$$

Equation (5) further reduces to our final model where terms are introduced representing the proportion of input energy used to create work though vaporization ($\boldsymbol{\sigma_1}$) and gas expansion ($\boldsymbol{\sigma_2}$) respectively.

(3.6)

$$\mathbf{S} = \frac{\mathbf{1}}{\boldsymbol{AB_nPf}}\left(\frac{\boldsymbol{Pv_g}}{\Delta \boldsymbol{H_{vap}}}\dot{\boldsymbol{Q}}_{\boldsymbol{in}}(\boldsymbol{\sigma_1}) + \dot{\boldsymbol{Q}}_{\boldsymbol{in}}(\boldsymbol{\sigma_2}) - \dot{\boldsymbol{W}}_{\boldsymbol{loss}}\right)$$

$$\dot{\boldsymbol{Q}}_{\boldsymbol{vap}} = \boldsymbol{\sigma_1}\dot{\boldsymbol{Q}}_{\boldsymbol{in}} \quad , \quad \dot{\boldsymbol{W}}_{\boldsymbol{gas}} = \boldsymbol{\sigma_2}\dot{\boldsymbol{Q}}_{\boldsymbol{in}}$$

The liquid vaporization is determined by the portion heat input into the liquid in relation to heat of vaporization $\Delta \boldsymbol{H_{vap}}$**.** A lower heat of vaporization leads to more vapor converted for a given heat energy. Therefore, we expect the heat of vaporization is inversely related to the amplitude.

3.3 Experimental and Model Results

The data collected from the vaporization experiments showed a clear increase in power output with decrease of latent heat of vaporization of the fluid used. The developed model shown in figure 3.3 demonstrates a strong agreement with experimental measurements. With an R^2 of 0.959, 0.999, 0.991 and 0.840 for the water, IPA, methanol, and ethylene glycol respectively. The results indicate that the model increases in its accuracy at lower heat of vaporizations.

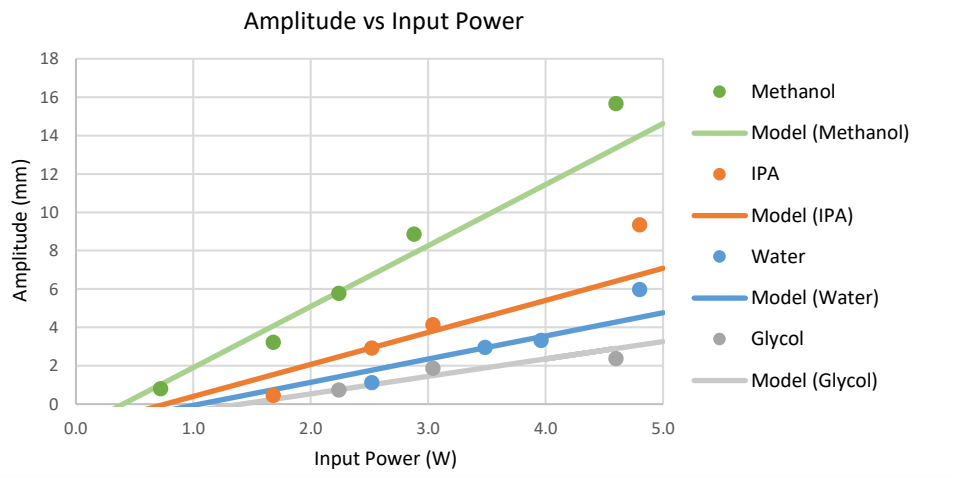

Figure 3.3: Performance analysis of different working fluids

The model and experimental results demonstrate that liquids with a lower enthalpy of vaporization produce a greater amplitude of oscillation due to the higher conversion rate of input energy into vaporization at a given hot column temperature.

Through use of mixtures with a range of vaporization pressure it, was also found that high vapor pressure produces the largest output (Figure 3.4A). It is assumed that regardless of the mixture, the engine frequency remains unchanged due to the identical geometry of the engine. It has been observed in work by our lab and others that the engine's operational frequency is geometry dependent and independent of input energy [1][12][29].

However, testing indicated that there was some dependence of frequency on the working liquid for the ethylene glycol mixtures (Figure 3.4B). Because ethylene glycol has a significantly higher viscosity than the other fluids used, there is likely some effect on these physical properties and the observed frequency change. Regardless, this factor is not explored in this study.

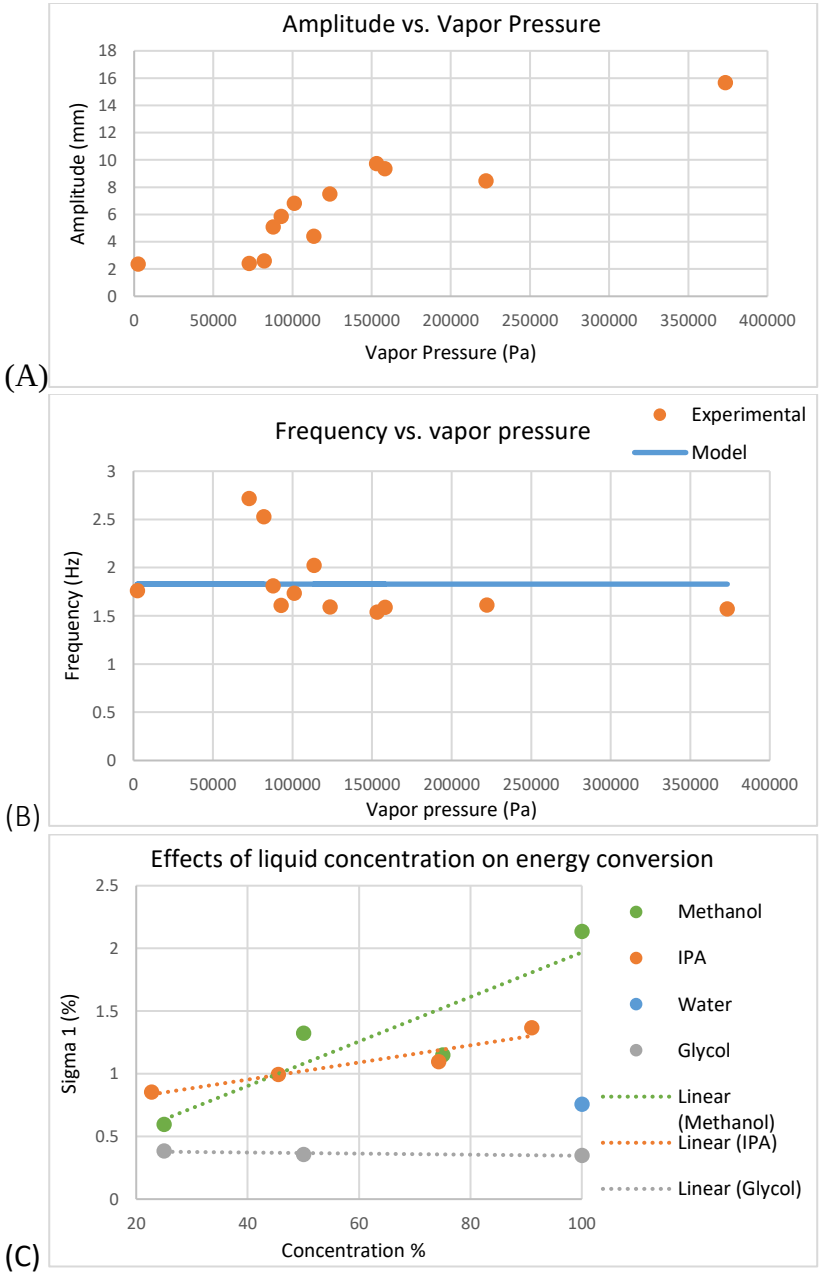

Figure 3.4: Liquid vaporization experimental and model results (A) Amplitude (B) Frequency and (C) Power output vs. heat of vaporization

The model was also used to determine the percent of total input energy contributed towards vaporization (σ_1) with regards to the concentration of the mixtures (Figure 3.4C). We assume that the liquid with the lower boiling point is the only fluid participating in vaporization within the mixture. The results indicate that as concentration of the lower heat of vaporization liquid increases, more energy can be converted to mechanical work.

The fitted model suggests that there is a strong correlation with power output of the engine and a high vapor pressure of the working liquid, for a constant temperature heat source. This is in congruence with results found by work performed by Markide's group in London which tested working fluids for a mechanical two-phase engine [3]. Our values of the percentage of input energy resulting in power generation from vaporization (σ_1) and gas expansion (σ_2) suggests that fluid vaporization is the primary driver in engine output.

Table 3.3: Proportion of input energy toward vaporization and gas expansion

Liquid	Vaporization (σ_1)	Gas Expansion (σ_2)
Water	0.67%	0.0045%
IPA	0.99%	0.0045%
Methanol	1.91%	0.0045%
Ethylene Glycol	0.60%	0.0045%

With σ_1 being two orders of magnitude larger than σ_2. This further contributes to the hypothesis that the gas expansion is not a significant driver in engine performance for the tested conditions. Through analysis of the free parameters it is also observed that the proportion of energy converted to vapor is more heavily depend on heat of vaporization than on input power.

4. Engine Cycle Analysis

To better understand the internal thermofluidic mechanisms which converts heat energy into work, data was collected and analyzed to understand the engine cycle both in the loaded and unloaded configuration. Though the dry air may be approximated as an ideal gas, because we hypothesized that vaporization of the working fluid is the driving factor contributing to the output of the engine, a more complex thermodynamic problem presented itself. To solve this problem, we first empirically analyzed the engine's cycle to model the temperature, pressure, and volume profile of the engine's gas chamber.

4.1 Apparatus

The engine constructed for the purposes of understanding the internal thermodynamic cycle was created to be 1/2" thick acrylic engines. However, additional holes were drilled to allow for the insertion 5 k-type thermocouples and one 1/8" tub for pressure sensor connection. The sensors were added to measure the internal working gas and liquid properties. The thermocouples and pressure sensor tubing were sealed using marine epoxy. Special care was taken when sealing the thermocouples as an early engine construction failed due to the thermocouples' insulative sleeves acting as wicks allowing both gas and liquid to escape from the engine chambers. Along with the sensors, a time readout digital display was incorporated with the engine so that pressure and temperature values could be properly correlated, with respect to time, to volume values found through video analysis.

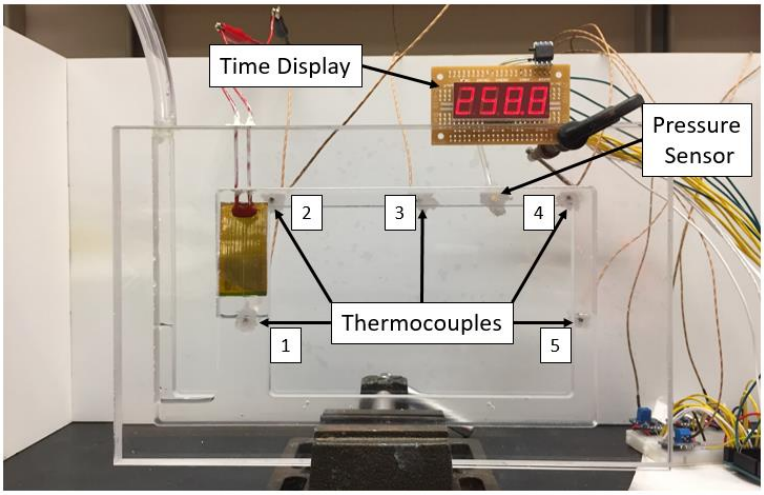

Figure 4.1: Cycle analysis engine

The temperature, pressure, and time data values were processed by an Arduino Mega and printed to the user's computer via the serial port monitor. Video analysis was performed via Tracker video analysis software. The engine design used for this apparatus may be found in Appendix (B).

A limitation involved with the data collection technique was the processing time required for the analog to digital conversion (ADC) of the thermocouples. Testing showed that a single thermocouple reading required 67 ms to be read and stored. With the high end of engine operation frequency being 3 Hz the Nyquist rate is 167 ms. Due the processing time required by the ADC, the microcontroller thus cannot successively record 5 thermocouple values without introducing aliasing into the individual thermocouples temperature profiles. The decision was made to instead process one thermocouple at time (over a 10s interval) and then to normalize the data over the engine cycle. It is assumed this is a valid technique as the engines operate with steady state amplitude and frequency, thus the internal temperature and pressure profiles should fluctuate in a steady state manner as well.

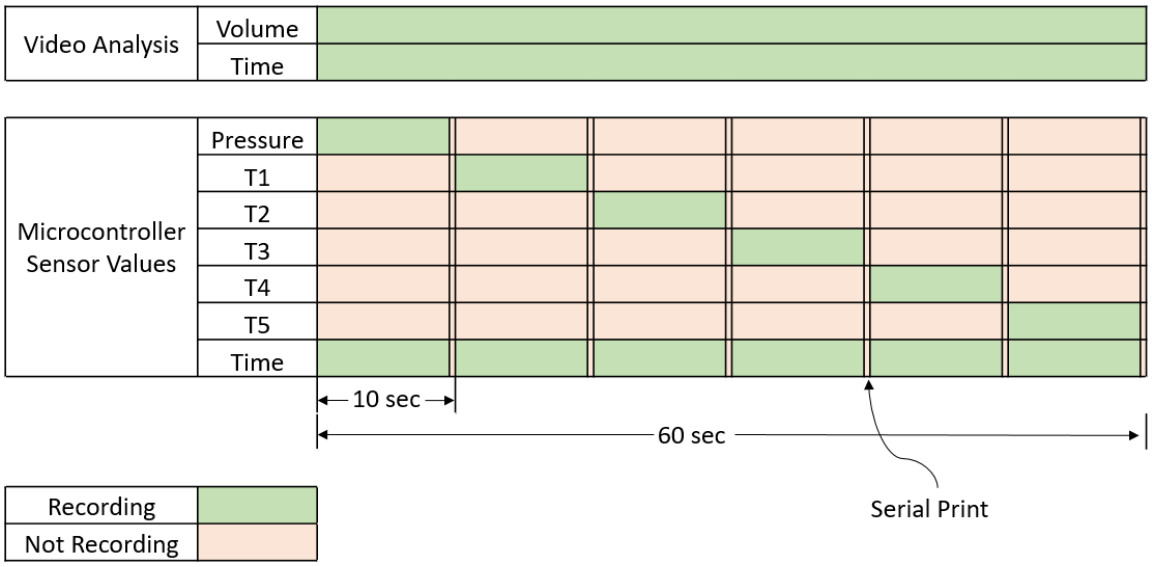

Figure 4.2 Block diagram of data collection process

The provided block diagram gives a visual explanation of the data collection process. Once the engine is found to be operating at a steady state (i.e. operational frequency and amplitude are unchanging over time) the 60 second data collection process may begin.

4.2 Results

The data analysis of the unloaded and loaded configurations demonstrate that the volume and pressure of the gas chamber fluctuates in phase with each other (Figure 4.3A and C). Data analysis also demonstrated that the temperature of the gas chamber fluctuates out of phase with chamber volume for both loaded and unloaded configurations (Figure 4.3B and D).

(A)

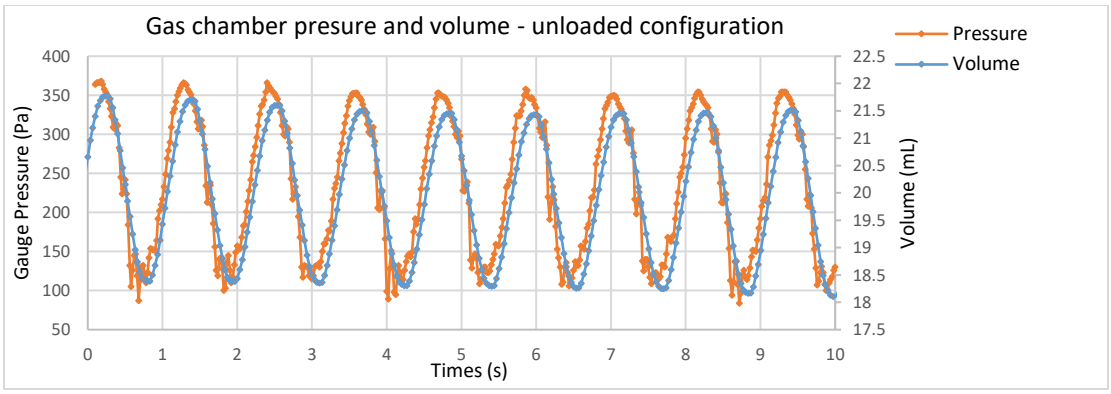

(B)

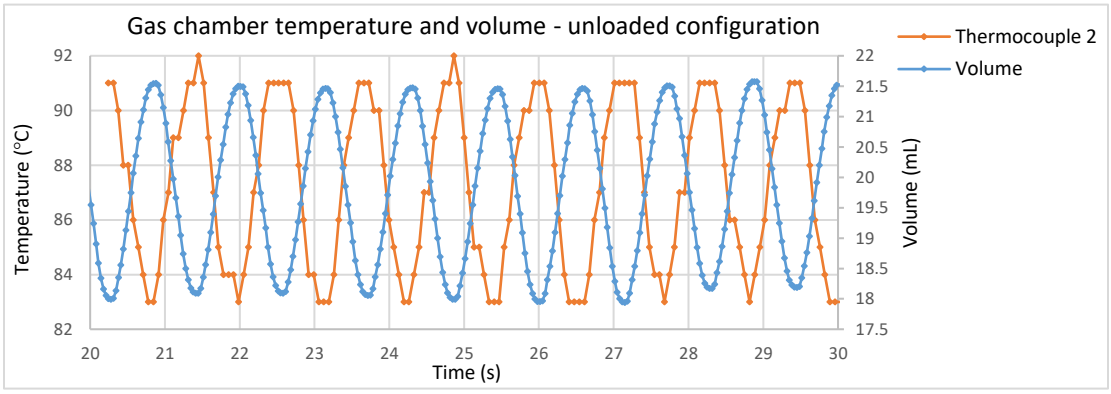

(C)

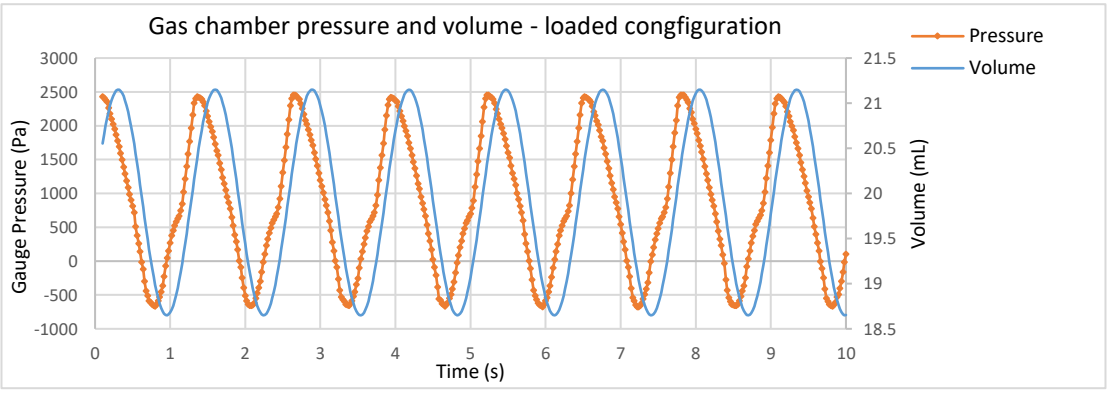

(D)

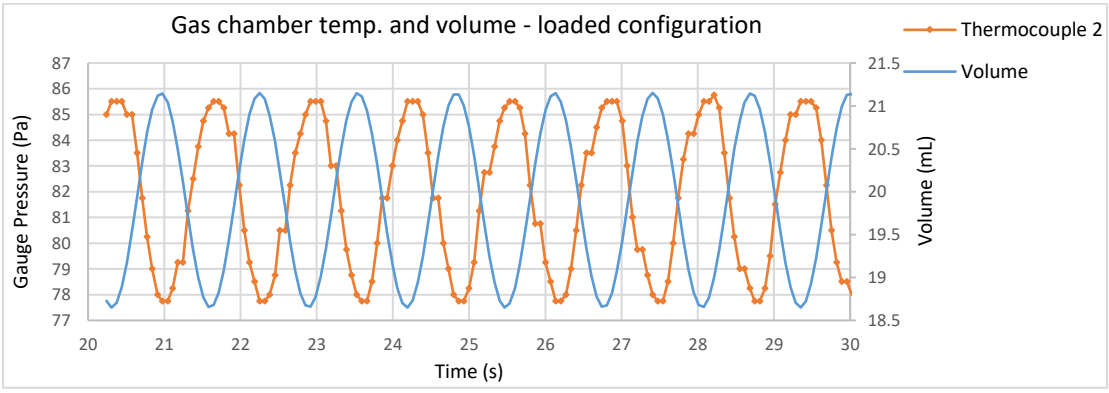

Figure 4.3: Pressure, temperature, and volume profiles
Unloaded chamber (A) pressure and (B) temperature profile
Loaded chamber (C) pressure and (D) temperature profile

When comparing the unloaded and loaded results: the most notable difference is that the loaded configuration operates with an order of magnitude larger pressure fluctuation. Additionally, the loaded configuration's temperature profile is more in phase with the pressure profile than with the unloaded configuration. Note that volume profile in figures 4.3C and D was a generated sine fit curve with stroke volume equal to the measured periodic output of the pump. Tracker software was used to determine the phase angle of the volume fitted curve with respect to the time display digital read out.

Along with the pressure, volume, and temperature profiles found with respect to time, the profiles were normalized with respect to the cycle.

(A)

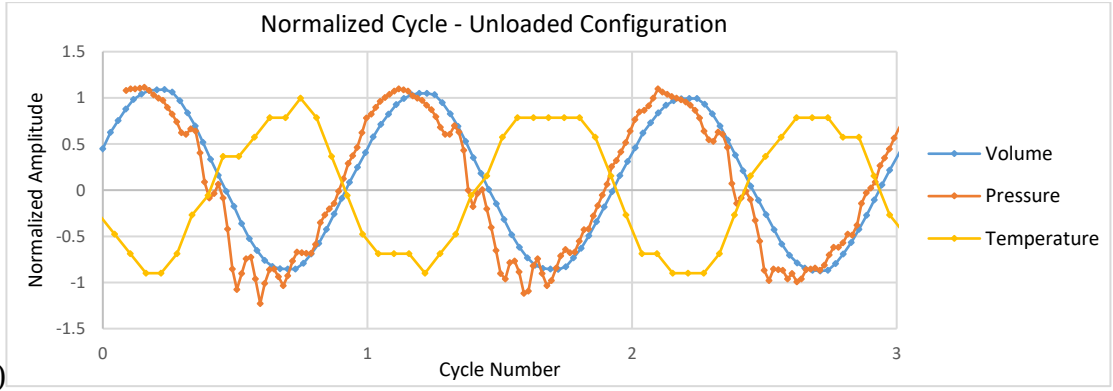

(B)

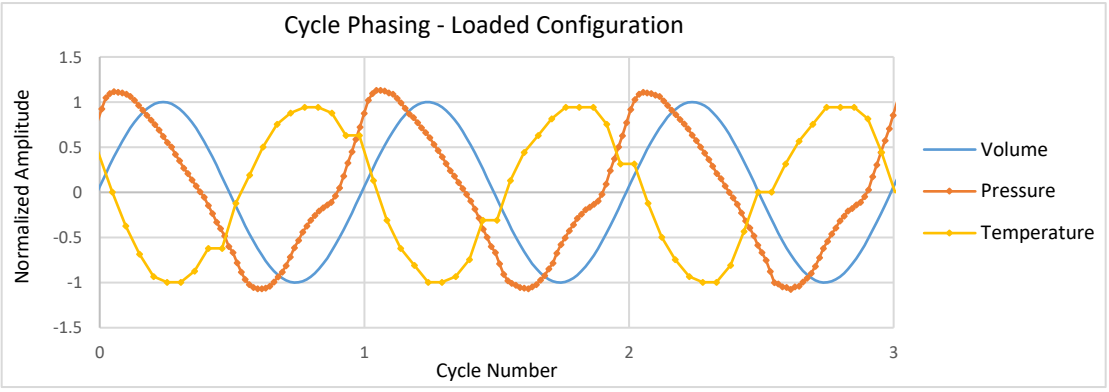

Figure 4.4: Normalized pressure, volume, and temperature of cycles
(A) Normalized pressure, volume, and temperature of the unloaded engine cycle
(B) Normalized pressure, volume, and temperature of the loaded engine cycle

The normalized plots (Figure 4.4) display the pressure, volume and temperature profiles for the unloaded and loaded configurations. The cycle number represents the period of the cycle with 1 cycle number correlating to a complete cycle. The vertical axis' normalized amplitude values represent the value of recorded data divided by the amplitude of that data's fitted curve. Figure 4.4A and B demonstrate that the temperature is out of phase with the pressure and volume profiles. This may be in part due to the vaporization of the water leading to increased mass in the system's gas-phase chamber. The phase shift can also be explained by the location of the thermocouple within the thermally dynamic system. The average temperature of the gas chamber may increase with the increased volume and pressure; but at the location of the thermocouple cooler gas may be shuttled across the temperature probe. This would explain the observed properties and demonstrate the importance in thermocouple locations when analyzing thermal systems.

4.3 Cycle analysis results

To analyze the cycle within the gas chamber PV diagrams were developed for the cycles.

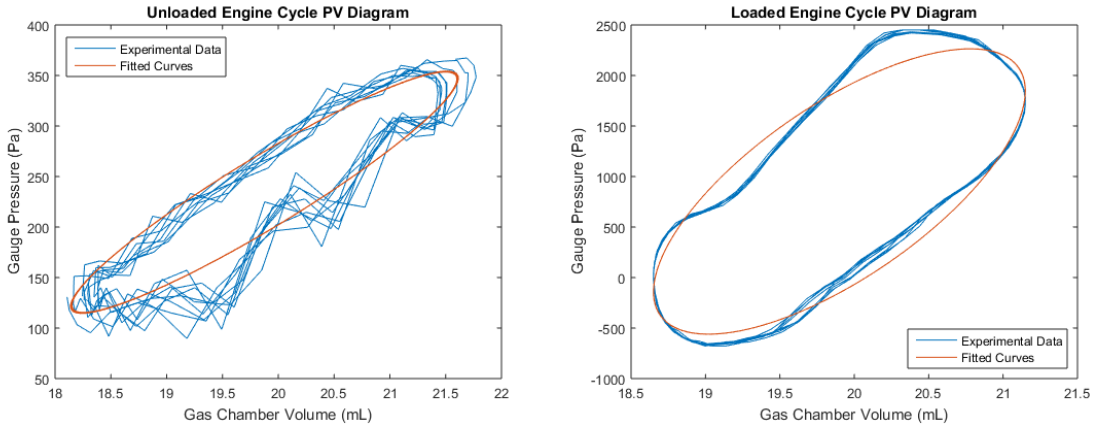

(A) (B)

Figure 4.5: Engine cycle PV diagram at 14.5 watts
(A) Pressure and volume diagram for the unloaded engine configuration
(B) Pressure and volume diagram for the loaded engine configuration

Note that the figure 4.5B demonstrates a ‘smoother’ profile, this is partially due to the loaded configuration’s curve fitted volume profile, but more so due to higher pressure fluctuations creating a less erratic signal.

The loaded configuration was analyzed in more depth to produce the following figure:

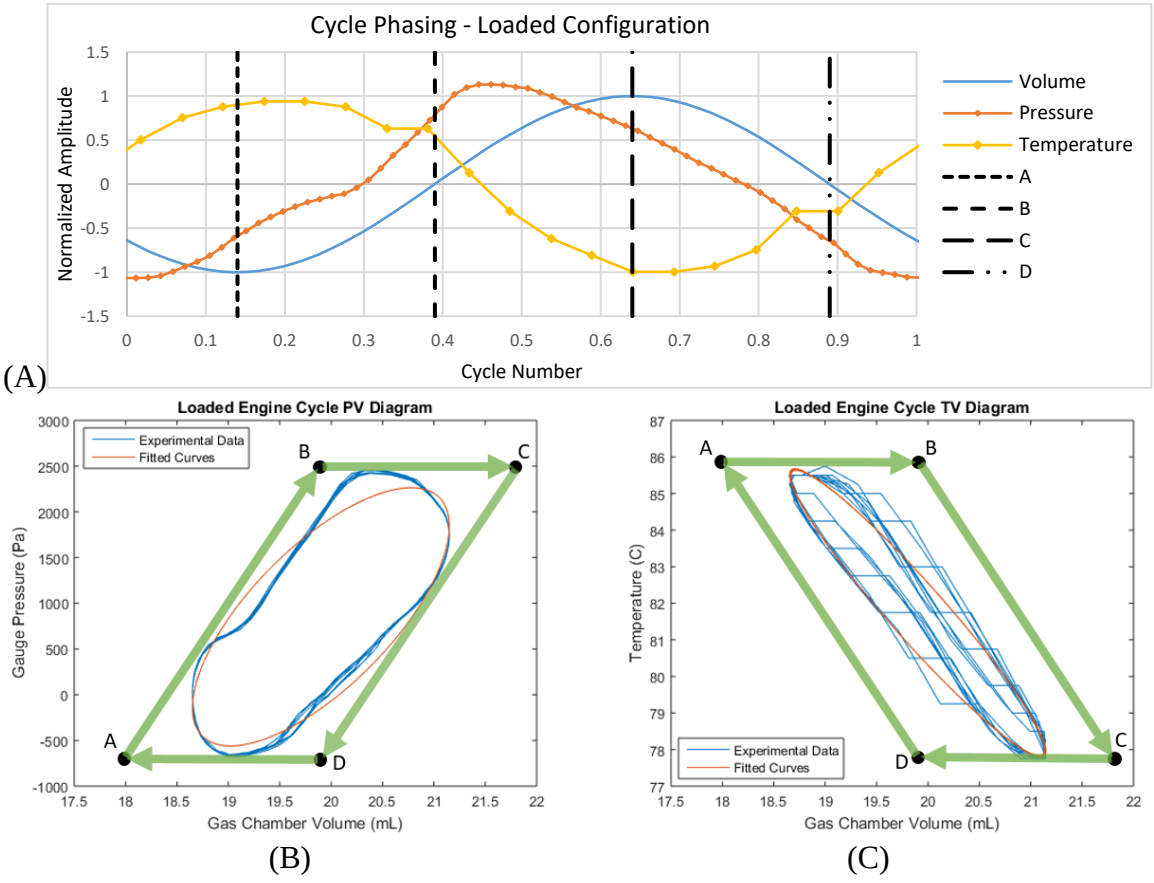

Figure 4.6: Engine cycle analysis
(A) Normalized pressure, volume, and temperature profiles of the loaded cycle
(B) PV diagram of the loaded cycle (D) TV diagram of the loaded cycle

Though not an ideal cycle, the engine gas chamber can be approximated with periods of isothermal states from points A to B and C to D, and adiabatic states from B to C and D to A. The isothermal heating/cooling processes can be explained by the phase change occurring at the constant temperature liquid-gas interfaces of the liquid pistons.

4.4 Vapor Contribution Analysis

In determining the fluctuation of the water vapor the following assumptions were made: The air within the chamber may be treated as an ideal gas, no gas escapes from the chamber during operation, the air and water vapor are in thermal equilibrium, and that operation pressure is close enough to atmospheric pressure that psychometric values of specific volume and humidity ratio may be used. It could also be safely assumed that pressure variation is negligible in volume calculations, due to its small variation in comparison to operating pressure, however because this data is available pressure variation has been included in the analysis.

Air mass was calculated through use of psychometric values at resting temperature. The resting engine volume was measure and assumed to be at 100% relative humidity as the measurement was taken place after operating the engine. The 'initial' gas chamber values are typically recorded after testing the engines, and letting them cool, as to ensure the humidity within the gas chamber as well as it allows for gas chamber calibration while testing. Through use of psychometric values, the ideal gas law, and Amagat's law of partial volumes the contribution that vapor change has on engine operation has become apparent [30].

$$m_{air} = \frac{V_{initial}}{v_g(T_{initial})} \ , \ V_{air} = \frac{m_{air}RT}{P} \ , \ V = \sum_i V_i \ , \ V_w = V - V_{air}$$

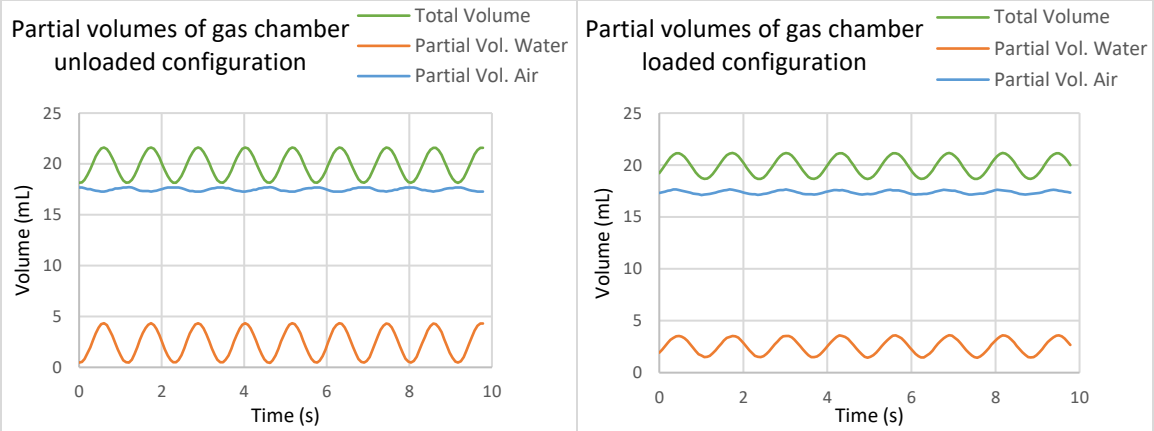

(A) (B)

Figure 4.7: Partial volume contributions to engine performance
(A) unloaded and (B) loaded gas chamber volumes with respect to composition

Figure 4.8 gives a clear demonstration that volume fluctuation in the gas chamber is due to vapor content, though the majority of the gas chamber volume is still made up of air.

4.5 Cycle Discussion

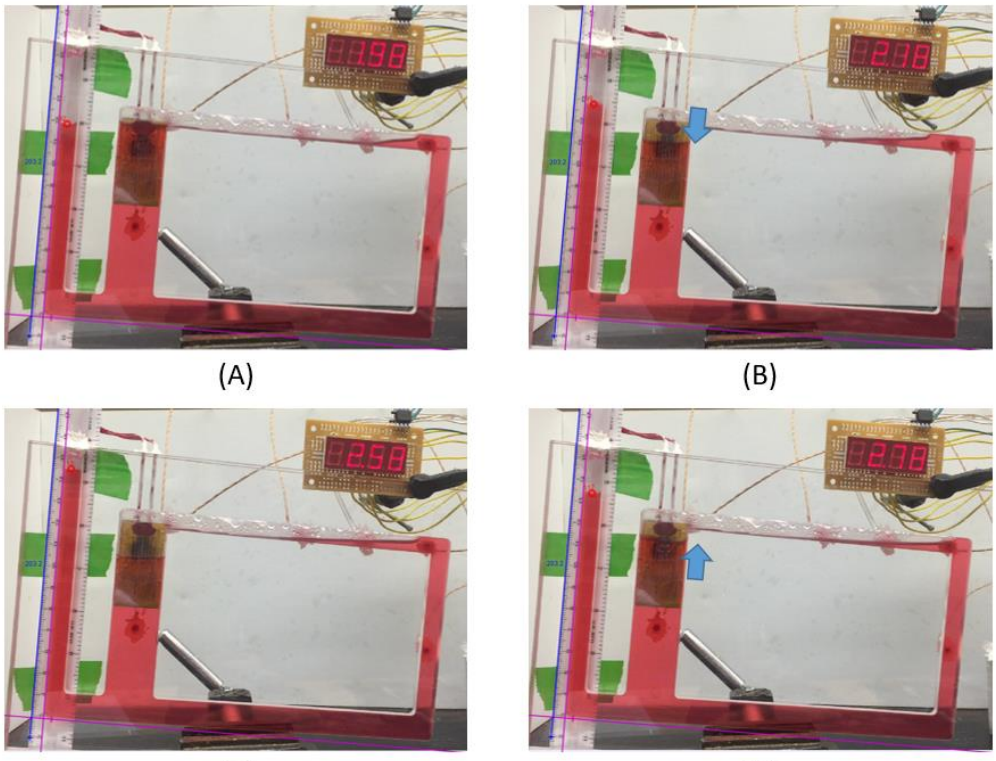

(A) (B)

(C) (D)

Figure 4.8: Engine cycle discussion

To explain the results from section 4.3 and 4.4 this section offers a qualitative discussion of the physical phenomenon occurring during the cycle. We begin at state A (Figure 4.9 and 4.10) at this point the hot column piston is located at top dead center (TDC). It is important to realize that, with Fluidynes, liquid connection between the hot cold columns is critical to operation. While the hot piston is at TDC the cold piston is observed to be at bottom dead center (BDC) (Figure 4.9A). Because the two pistons are at a height differential there is also a pressure differential that drives the hot piston down and the cold piston up. As the hot column travels from state A to B, a relatively high amount of energy is being transferred into the fluid contributing towards vaporization. Because temperature is unchanging during phase transition this vaporization period is said to be *isothermal heating*.

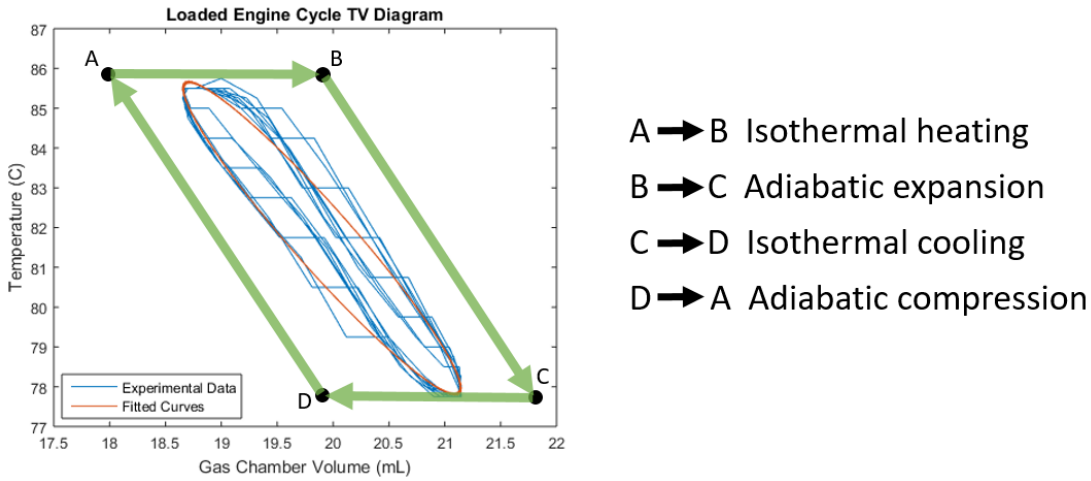

Figure 4.9: TV diagram of engine cycle

As the hot piston continues to drive downward from state B to state C the vaporized water expands producing useful output work as well as adds restorative force to the dynamic piston motion. As the hot column piston moves downward to BDC the heater becomes more exposed to the gas-phase portion of the system, thus significantly lowering

the overall heat transfer coefficient. Because of the vapor expansion and relatively low convection the process is approximated as *adiabatic expansion*.

At state C the pressure differential created by the height difference in the columns is able overcome the momentum of the fluid. As the hot column moves upward from BDC and transitions from state C to D the majority of the heater remains exposed to gas-phase. Thus the primary thermodynamic mechanism driving this process is the condensation occurring at the cold column liquid-gas interface. This condensation is said to be *isothermal cooling*.

Note Figure 4.11 demonstrates the normalized thermocouple temperature read outs where T4 represents the liquid-gas interface of the cold column.

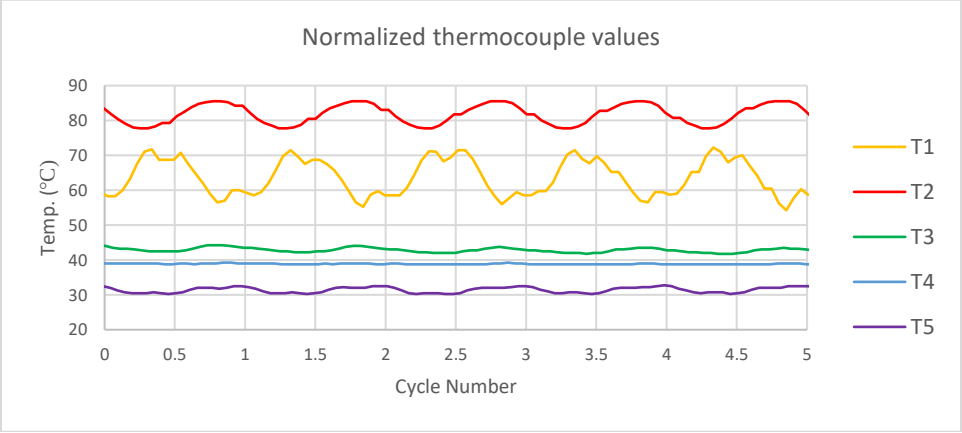

Figure 4.10: Normalized temperature profile of engine thermocouples

Because temperature is observed to be unchanging at the interface of cold column (Thermocouple 4) and is held at 100°C at the liquid-gas interface of the hot column: the cooling (condensation) and heating (vaporization) of the water is said to be isothermal.

During the final transition from state D to A the momentum of the fluid brings the liquid piston to TDC of the hot column. During this transition the condensation of the

water vapor leads to compression of the gas chamber. This process is approximated to be *adiabatic compression*.

4.6 Chapter Discussion

With consideration of both the liquid and gas portion of the engine cycle a full conceptual understanding of the engine cycle is provided. The results from this analysis along with the results of chapter 3 offer overwhelming evidence that the primary driver in the engine is not the gas Stirling cycle but rather a vapor cycle.

Table 4.1: Comparison of liquid piston and Stirling cycle

Liquid piston heat engine	Stirling engine
Isothermal heating	Isochoric heating
Adiabatic expansion	Isothermal expansion
Isothermal cooling	Isochoric cooling
Adiabatic compression	Isothermal compression

When comparing the proposed liquid piston engine cycle with the Stirling cycle it can be said that the processes are distinctively different. With a physical understanding, supported by collected data, the phase change of the water can be said to occur in an isothermal manner. By considering the water transition between states of vaporization and condensation the cycle may be broken into states of isothermal cooling/heating and adiabatic compression/expansion. The processes undergone by the liquid/vapor water traveling through the system offer a revealing approximation of the engine cycle.

By better understanding the two-phase cycle occurring within the engine, techniques may be established to better optimize the system. Through this simple explanation of the engine cycle a better understanding of engine operation has been achieved.

5. Geometry Effects

Several tests were conducted to better understand the effects that geometry plays on work output of the engines. These tests aimed to isolate the influence of engine, height, length, depth, and scalability. Through this study we postulate that spacing between hot and cold columns can be optimized by considering the heat boundary and viscous losses.

5.1 Effects of height and length

The first of these experiments performed involved the engine height and length. For this experiment 8 engines were constructed varying in height and length. The test group involved 5 engines with common displacer height and variable length. The second test group involved 3 engines with common displacer length and variable height.

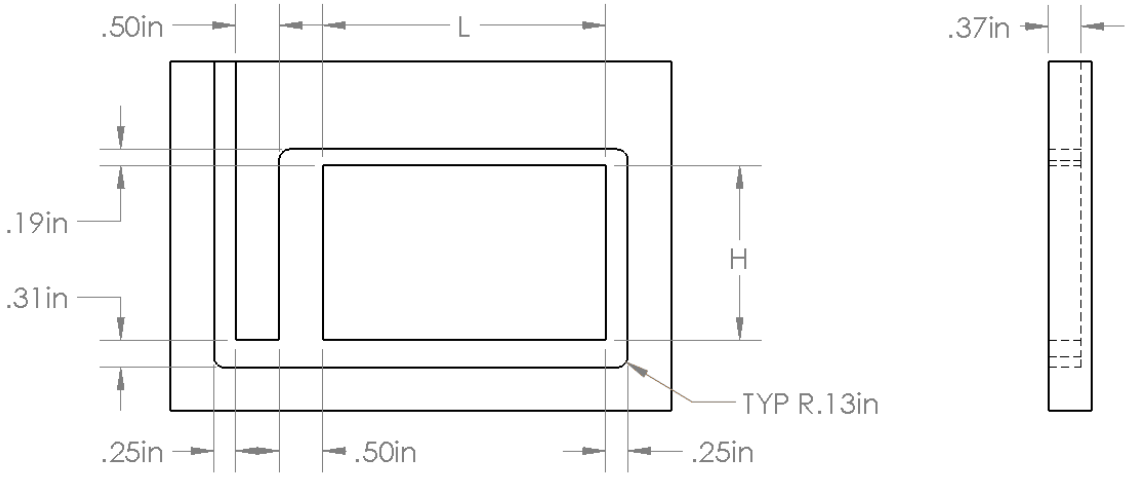

Figure 5.1: Engine geometry with varying length and height

The height and length of the engines used as seen in table 5.1 were chosen as they stayed within typical range which these engines have been tested.

Table 5.1: Lengths and heights of engines tested

	Height (in)	Length (in)
Varying Length	2	0.75
	2	1.75
	2	3.25
	2	4.75
	2	6.25
Varying Height	1	3.25
	2	3.25
	4	3.25

The engines were tested at an input power of 4 Watts and the engine performance data sets were collected via Tracker video analysis.

The results from varying the column spacing length demonstrate the following trends. As engine length increases so too does amplitude, up to characteristic length, after which amplitude begins to decrease with further increasing of engine length (Figure 5.2A). As engine length increases frequency decreases, though at lesser rate after the characteristic length is reached (Figure 5.2B). The varying column spacing (length) demonstrated a maximized engine performance within the middle of the range tested (Figure 5.2C).

The results from the column height testing demonstrate that though the change in geometry influences the performance, the significance created by the changing height was not as dramatic relative the change in column spacing (Figure 5.2F). The results from testing both the engine height and length thus lead to the development of the vapor entrance theory for wet Fluidynes.

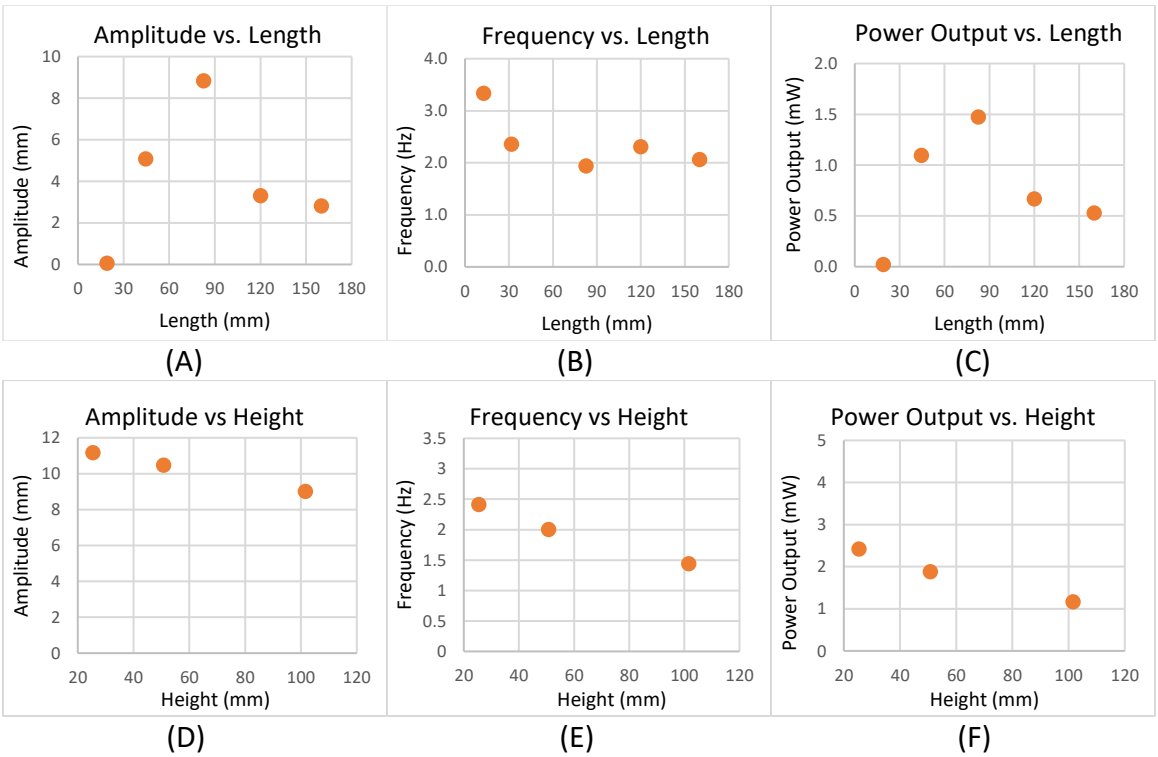

Figure 5.2: Performance results of varying lengths and heights
(A) Amplitude, (B) frequency, and (C) power output of engines with varying lengths
(D) Amplitude, (E) frequency, and (F) power output of engines with varying heights

5.2 Vapor Entrance Theory

Based on the concept of thermal entry length, it is assumed that magnitude of the temperature gradient decreases with increased column spacing, but only up to a certain distance defined as the thermal entrance length [28]. The vapor entrance theory postulates that the column spacing effects engine performance due to the volume of liquid vapor that is vaporized into the gas chamber.

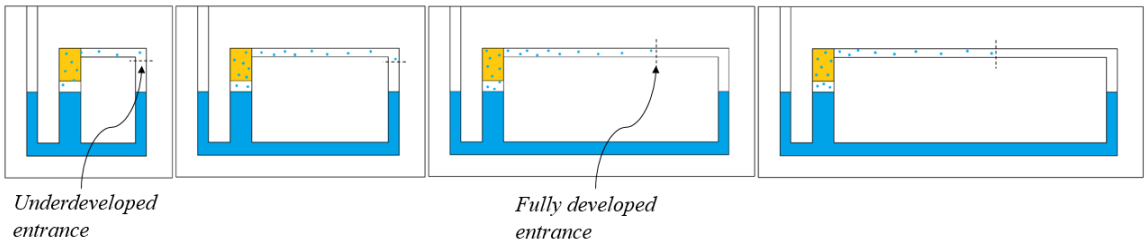

Figure 5.3: Vapor entrance at varying lengths

As the column spacing increases so too does the potential volume of liquid vapor to enter the air chamber. However, due to the understanding of thermal entrance, the increase in length will only effect the temperature profile of the inlet up to certain distance. After this characteristic distance is reached, the water vapor will begin condensing and no additional vapor contributes to volume change. This thus separates the engine lengths into two regimes of underdeveloped or fully developed vapor entrance (Figure 5.3).

In Figure 5.2A we observe that amplitude increases with engine length up to a maximum of 80 mm, after which amplitude decreases. We postulate that, for our engine height and input power, the space exceeding 80 mm does not affect the temperature profile of the thermal entrance. Because no additional liquid vapor is absorbed in the air chamber past this length, the maximum steam contribution to amplitude remains constant (Figure 5.4A). However, additional engine length past this characteristic distance does contribute to additional viscous drag (Figure 5.4B).

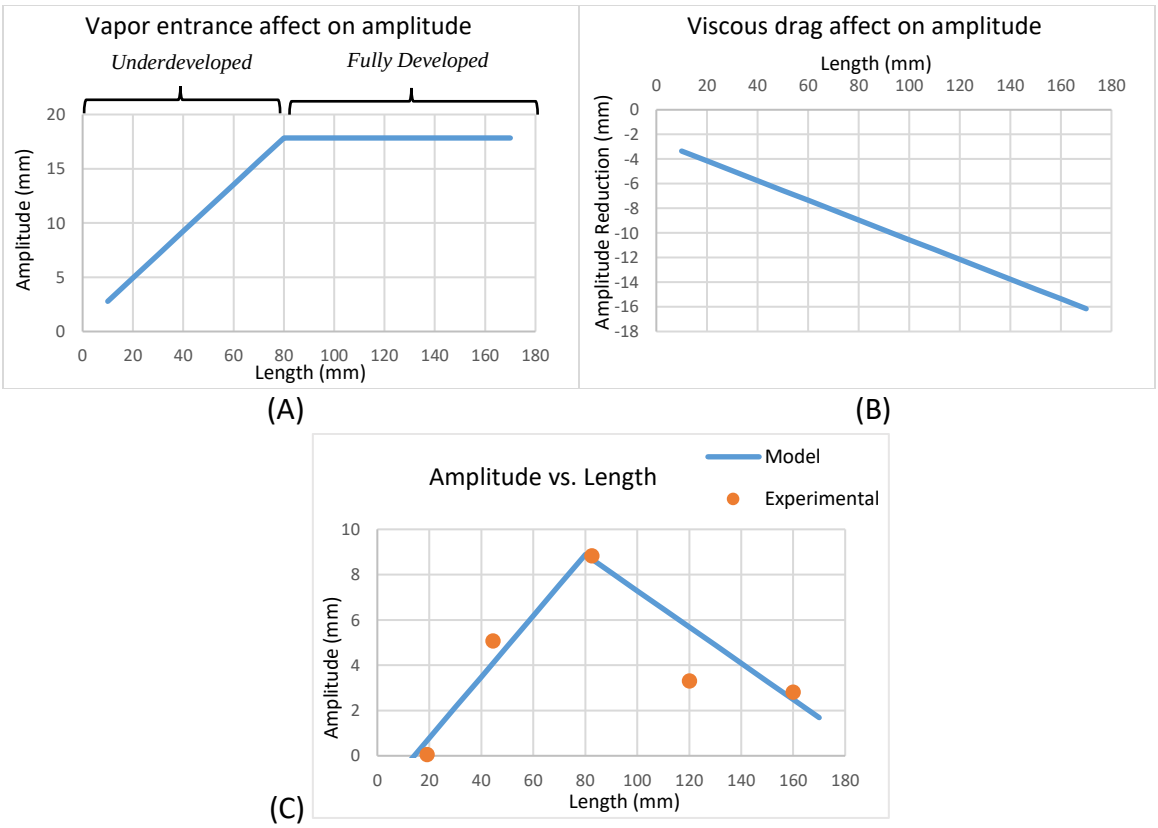

Figure 5.4: Effects of vapor entrance and viscous drag on amplitude (A) Contribution of vapor volume on amplitude (B) Amplitude loss due to viscous drag (C) Combined factors of vapor volume and viscous drag on amplitude

The relationship between amplitude and vapor entrance is described by the linear equation (5.1), in which $\boldsymbol{S_{vap}}$ is the vapor contribution to amplitude and **L** is the air column length. The function contains a linearly increasing amplitude within a column spacing range of 0 to 80 mm and remains constant above 80 mm.

$$\boldsymbol{S_{vap} = \begin{cases} C1 * L + C2 & 0 < L < 80\ mm \\ S_{vap}(80) & L \geq 80\ mm \end{cases}} \quad \textbf{(5.1)}$$

C1 represents the slope for the linear increase in engine amplitude with length due to this increase in potential steam production. Where $\boldsymbol{h}$ is the hydraulic head driven by the Darcy-

Weisbach friction factor $\boldsymbol{f_D}$ for pipes in laminar regime, the hydraulic head can be expressed as:

$$\boldsymbol{h = f_D\left(\frac{L}{d}\right)\left(\frac{V^2}{2g}\right)} \quad \textbf{(5.2)}$$

By neglecting the relatively small changes in flow velocities [15] a linear friction factor can be assumed leading to the following fitting equation for the head loss due to viscous drag forces ($\boldsymbol{S_{vd}}$) relative to displacer length.

$$\boldsymbol{S_{vd} = C3 * L + C4} \quad \textbf{(5.3)}$$

The fitted result of both the vapor entrance effect and viscous drag after regression is as followed.

Table 5.2: Vapor entrance fitting parameters

C1 (unitless)	C2 (mm)	C3 (unitless)	C4 (mm)
0.2151	0.63	-0.08	-2.552

The proportional increase in amplitude due to engine length is determined by C1. Since the viscous drag is proportional to the pipe length and drag negatively impacts the operation of the engine: we find a negative C3 specifying the viscous head loss per unit length. Figure 3D compares the experimental and modeling data under the effect of air column spacing change. The model combines both viscous drag and thermal entrance (Figure 5.4C). This combination demonstrates that amplitude increases as air column length increases and reaches peak at 80 mm due to an increase in potential steam generation. The amplitude then decreases as thermal entrance effect remains constant but viscous effect keeps increasing its linearly negative effect on amplitude.

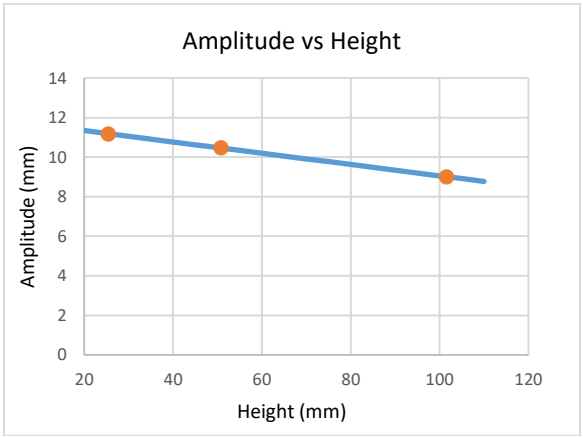

Figure 5.5: Height variation's impact on amplitude

Because changes in the fluid velocity are seen to be negligible within the engine, viscous drag is predicted to have a linear correlation with increased distance for the working liquid to travel. Therefore, the greater the engine column height, the larger the amount of head loss per cycle, and the smaller the amplitude. A linear function for engine height's impact on amplitude is proposed.

$$S = -C7 * H + C8 \qquad H > C8 \tag{5.4}$$

C7 represents the viscous drag proportionality constant between total head loss and engine height. C8 describes the upper limit of amplitude for minimal mechanical energy loss in the working fluid, and is explicitly not a function of engine height. Note that maximum stroke volume cannot be greater than the cold column volume.

Table 5.3: Engine height amplitude equation fitting parameters

C7 (unitless)	C8 (mm)
0.02854	11.91

From the fitting result, C7 is found to be small, which demonstrates that increased head loss per unit length of column height is a small factor in this engine. This result is realistic

considering the slow flow speed and small pipe roughness [8]. The upper limit of C8 is 11.91 mm (Figure 5.5).

5.3 Power Output Analysis

Figure 5.6A and B demonstrate the power output with respect to engine length and height respectively.

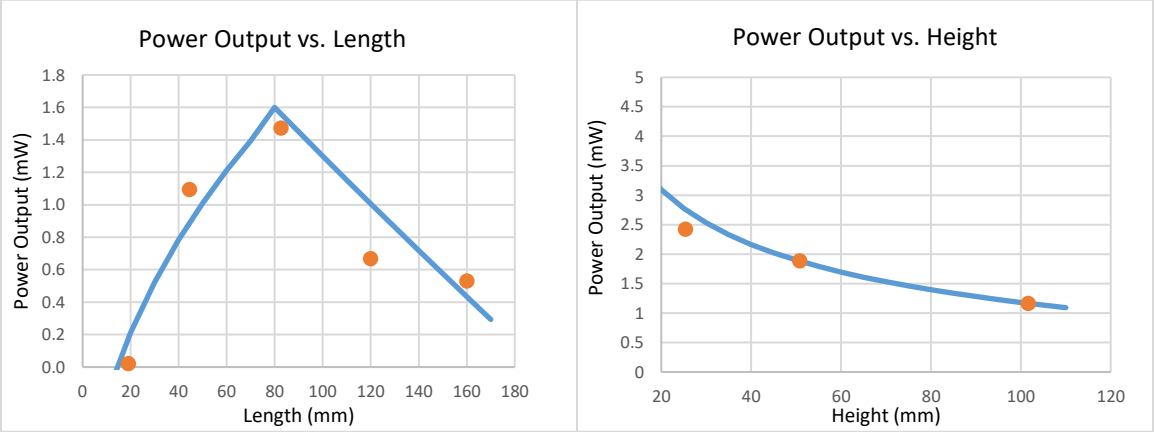

(A) (B)

Figure 5.6: Power output model with respect to length and height
Engine power output with respect to length (A) and height (B)

Results from the height and length analysis demonstrate that an engines performance can be maximized by using a minimal column height in congruence with an optimized column length with regards to the vapor entry.

5.4 Parameter optimization

When considering the optimal parameters for engine design several factors should be accounted for. Working liquid, engine length and engine height are controllable factors which have been explored in this research. Though input energy was explored, the effects of temperature differential was not explicitly researched.

Results from the vaporization study show that optimal output can be achieved by using liquid with high vapor pressure and low heat of vaporization. This agrees with Markides group which suggested ammonia and hexane as optimal liquids for their mechanical two-phase oscillator [3]. Note that safety and intended application should, of course, also be consideration. Safety considerations was, in part, why these fluids were not explored for these small engines which have educational applications.

Analysis from the height and length research indicate that performance of these engines can be optimized through careful consideration of their geometry parameters. Results indicate the performance can be optimized by minimizing column height so that stroke volume matches cold column volume. When determining engine length, the vapor entrance theory suggests that an optimal length can be achieved by maximizing vapor volume contribution and minimizing viscous drag. Note that temperature differential and thus the total input energy will affect both the vapor entrance length and the total stroke volume (i.e. optimal length and height). Intended operation temperature differential should thus be determined early in the design optimization.

A factor which was not explored in this research, that may lead to further optimization, is the initial volume of gas within the gas chamber as well as the composition of the gas. Another factor which was not explored is the potential of delivering pulses of energy into the heater to maximize different stages of the cycle.

6. Novel Applications

Along with performing quantitative research on engine performance a great deal of effort was expended in developing potential applications for the simple engine. This chapter examines several novel approaches possible with engine designs. Though the engines do not currently perform with efficiencies and power output demonstrated with conventional pumps, there are advantages to the simple design that can be applied to solve known problems. Thus, improvements and discoveries of liquid piston heat engine applications may further expand the potential in waste heat processing.

6.1 Flexible and Bendable Waste Heat Powered Pumps

With the excitement generated by flexible and bendable electronics and sensors, there is currently no approach demonstrated for a truly flexible, waste-heat powered pump. Such a pump may have applications for the cooling of dynamically moving objects. A design that can solve this problem is constructing an engine from flexible and elastic materials such as polydimethylsiloxane (PDMS) instead of stiff acrylic. The PDMS flexible engines offer added benefits in their ability to be rapidly manufactured and withstand higher temperatures than that of the acrylic engines.

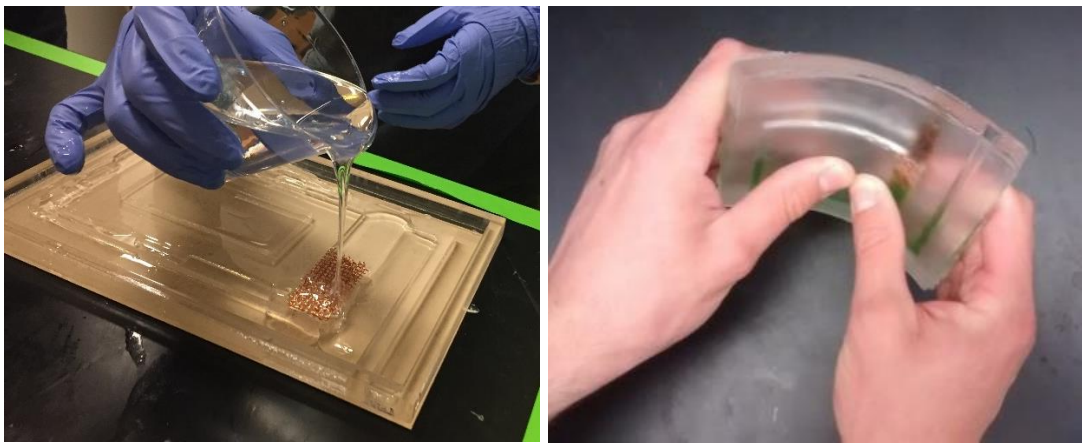

Figure 6.1: The flexible liquid piston engine
(A) Pouring PDMS elastomer into engine mold (B) Flexible engine deflection

6.1.1 Engine Construction

To construct the engines, two acrylic molds are milled to complete each part: one mold for the front side with impressions for the cylinders and another for the flat back panel of the engine. The engines are cast in two parts in PDMS elastomeric polymer. PDMS is mixed, poured into each mold, and cured at 120° C. It is during the pouring step that a copper mesh may be integrated in the hot column for external heat collection (Figure 6.1A). Else, a resistive heating element is adhered in the same manner as the acrylic engines. After curing individually, the two molded pieces are then bonded together through compression and heating. For these characterization studies an integrated resistive heater was included within the hot column for initial testing.

6.1.2 Testing and Results

The engine performance was first tested in an unbent, unloaded configuration to compare with the standard acyclic engines.

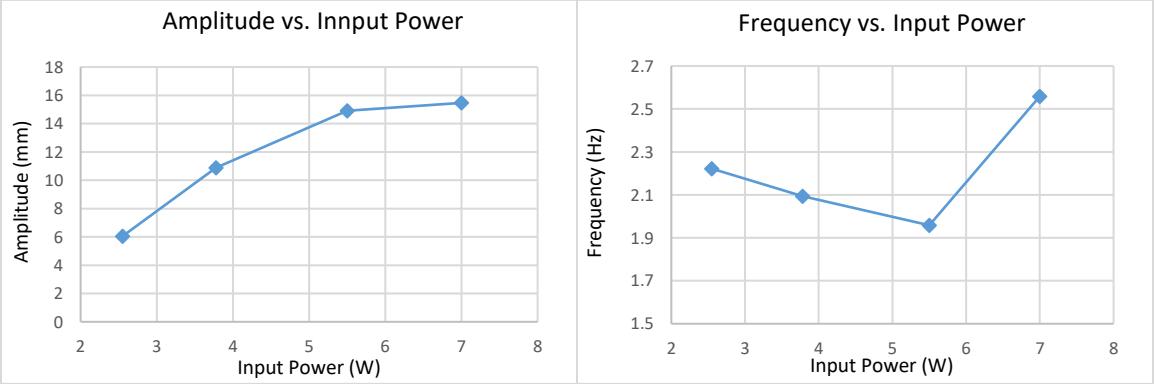

Figure 6.2: Unbent unloaded performance of flexible engine
(A) Amplitude and (B) frequency of the unbent engine at variable input powers

The amplitude of average steady state oscillation increases with the input power, from 6mm at 3 Watts up to 15.5mm when operating at 7 Watts. We did not exceed a maximum input

heat of 7 W to avoid damage to the polymer engine. The operating frequency was observed to change at high input powers (Figure 6.2A). The change in frequency is uncharacteristic of observations with rigid engine designs [1]. This change in frequency could be explained by the observation that the flexible materials may bow during operation, particularly at higher temperatures, changing the internal geometry thus resonance frequency of the system.

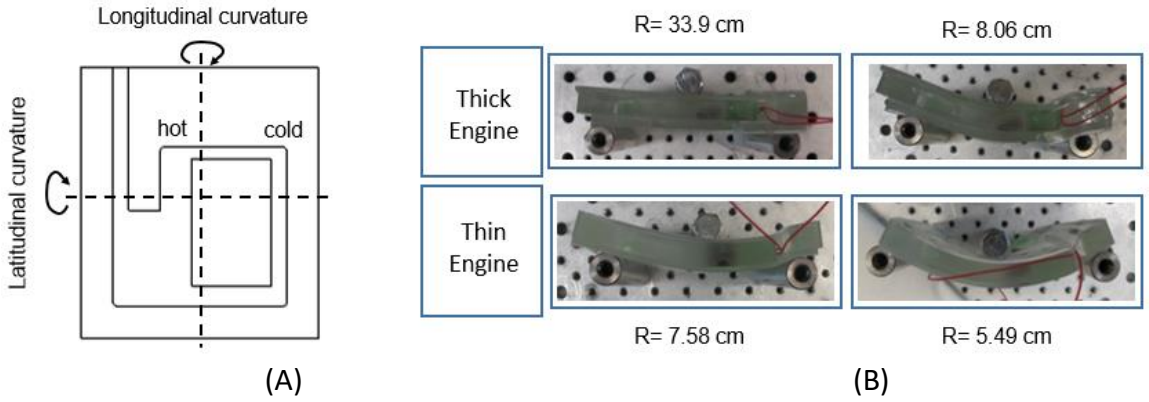

Figure 6.3: Bending characteristics of the flexible engine
(A) Longitudinal and latitudinal axes of curvature
(B) Aerial view of longitudinal bending

The flat design of the engines allows for flexing along 2 axes planar to the engine's face. The engines were tested and were successful in pumping water while bent along both longitudinal and latitudinal axes (Figure 6.2A). The engine performance was tested while applying longitudinal bending to both a thick and thin model of the engine. Aerial photographs of the testing setup for longitudinal bending is shown in Figure 6.3B for both the thin and thick engines. The bending was imposed by three lines of contact and the curvature was measured by defining a radius of a circle with the same curvature.

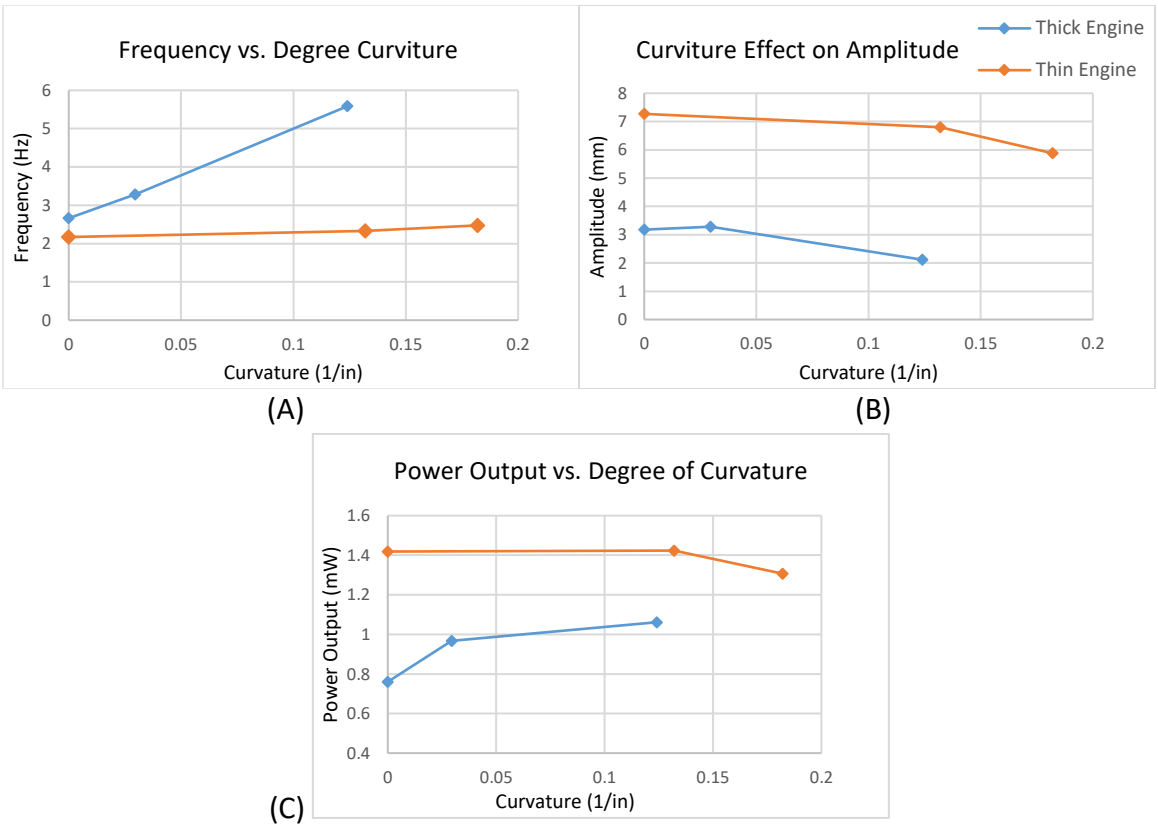

Figure 6.4: Thick and thin engine performance with longitudinal bending (A) Frequency, (B) Amplitude, and (C) Power Output of thick and thin engines at variable curvature

The oscillation amplitude was found to decrease with increasing curvature for both longitudinal bends (Figure 6.4B). In contrast, the oscillation frequency increased when bent (Figure 6.4A), resulting in an overall output power increase with the thick engine (Figure 6.4C).

6.1.3 Flexible Pumping

The flexible Engine could pump while in both the bent and unbent configuration, however the pump system was observed to produce less work while the engine was in a bent configuration. The thin flexible engine was used to produce the pumping results overcoming 2 cm head in an unbent and latitudinal bent configuration.

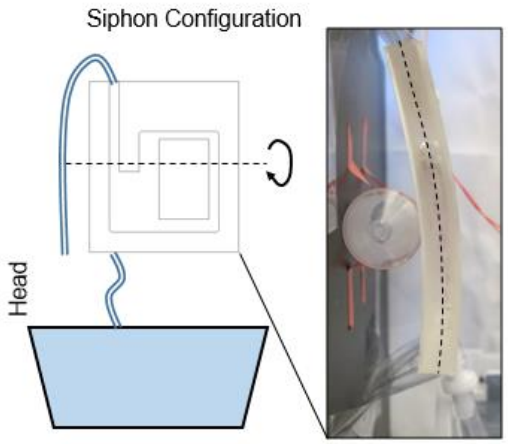

Figure 6.5: Flexible pumping configuration

Table 6.1: Thin flexible engine pumping results

Curvature (1/in)	0	.11
Pumping Flow Rate (mL/min)	7.4	4.0

Though less affective by 53% the resulting values demonstrate that the flexible engine can produce useful work while in a bent formation. To examine why the curved configuration would lead to a decrease in usable work, we performed FEA to examine the change in the cross-sectional area of the engine gas volume. The decrease can also be attributed to increase in internal fluid friction due to a relative increase of the liquid surface area contact to liquid column volume ratio.

6.1.4 Finite Element Analysis

A limitation to decreasing the bending modulus is that the engine walls should be sufficiently stiff to remain unyielding to pressure variations that occur during the cycle within the working gas. To examine the limitations of bending in the engine, we utilized finite element analysis (FEA) simulation software (Abaqus) to compute the internal stresses and strains within the engine during bending. The engine structure was imported from the CAD drawing with the effects of the liquid water ignored. The PDMS material was modeled as a planar, axisymmetric mesh. The boundary conditions were modeled as

three rigid bodies which contact the PDMS mesh during simulation. To capture the hyperelasticity of PDMS during the large deformation of our experiments, we used the Mooney-Rivlin model which is appropriate for elastomers materials undergoing large deformations [31]. For incompressible hyperelastic materials, the model derives the stress-strain relationship from the expression

$$W = C_1(I_1 - 3) + C_2(I_2 - 3)$$

where $\boldsymbol{W}$ is the strain energy function, $\boldsymbol{I_1}$= trace($\boldsymbol{G}$), and $\boldsymbol{I_2}$=(trace($\boldsymbol{G}$)-trace($\boldsymbol{G}^2$))/2, with $\boldsymbol{G}$ as the right Cauchy-Green deformation tensor. $\boldsymbol{C_1}$ and $\boldsymbol{C_2}$ are material constants, which were obtained by fitting the experimental force versus indentation curve of the 90-nm-thick film and then input into Abaqus to model the other thicknesses. The imposed curvature used in the simulation were identical to the experimentally tested conditions. The failure stress of PDMS is reported to be 2.29 MPa [32].

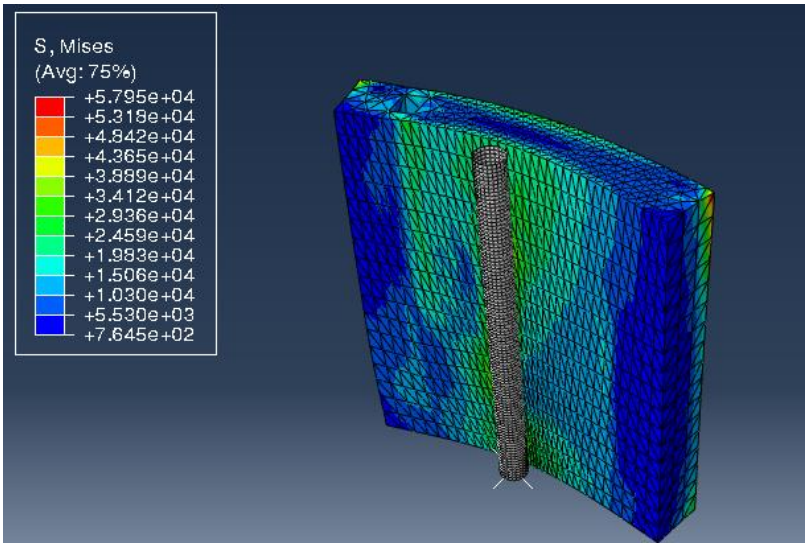

Figure 6.6 FEA analysis of flexible engine

To explain the observation of increased strain in thicker engines when bent, we note that increased strain results from increased distance of the neutral axis of the engine material

when curved. We find however that thin engines limit the efficiency of power generation, which scales approximately as the volume of the working gas. Moverover, viscous damping forces increase dramatically as the resistance of flow in a tube is proportional to the thickness of the tube. The need for flexible walls that remain unyielding to internal pressure has led to the conclusion that high bendability can be accomplished using thin, high modulus materials.

6.2 Solar Powered Engines

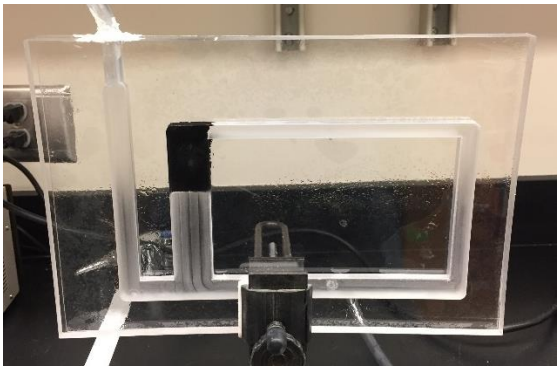

Figure 6.7: Solar Engine

Engines that were powered by light were created and tested to evaluate the efficiency of convert incident radiation to mechanical work.

6.2.1 Solar Engine Testing

The solar engines are constructed in the same manner as the standard acrylic engines with the exception that solar absorbing paint is applied to the hot column as opposed to using resistive heating elements to more fully convert incident radiation energy to thermal energy transferred to the working fluids (Figure 6.6). The engines are tested using a 375 W heat bulb and aluminum radiation shields. The radiation shields help to isolate the incident radiation on the hot column's heater (Figure 6.7A) as well as protect the cold column from heating, thus maintaining the necessary temperature differential. Note: a small gap is made between the engine and the radiation shield using air to insulate the engine from conduction of the radiation shield (Figure 6.7B).

(A) (B)

Figure 6.8: Radiation shield
(A) Radiation shield to isolate input energy on the heater
(B) Air gap created to insulate engine

6.2.2 Intensity Test Results

The following results show increasing the bulb distance, a proxy for intensity, from the engine decreases the engine performance. This experiment was performed by measuring steady state output column oscillation at variable distances between the engine and bulb. The bulb distance began at 15 cm from the engine and was increased by 2 cm increments per recording. Trials were performed with a 10 min delay to allow for steady state to be reached. The process was repeated until incident radiation no longer created oscillation with the engine (25 cm).

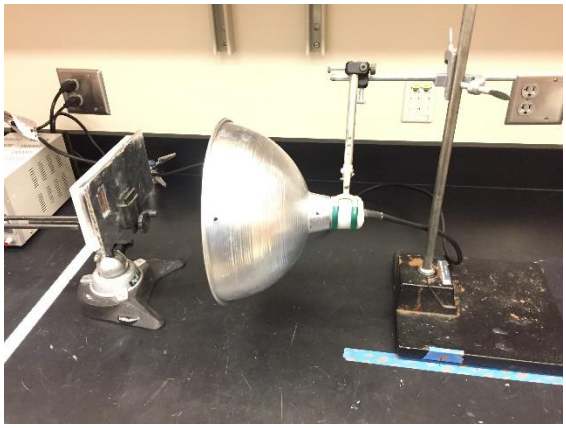

Figure 6.9: Intensity test apparatus

The following graphs show the results of the intensity test measured as bulb distance.

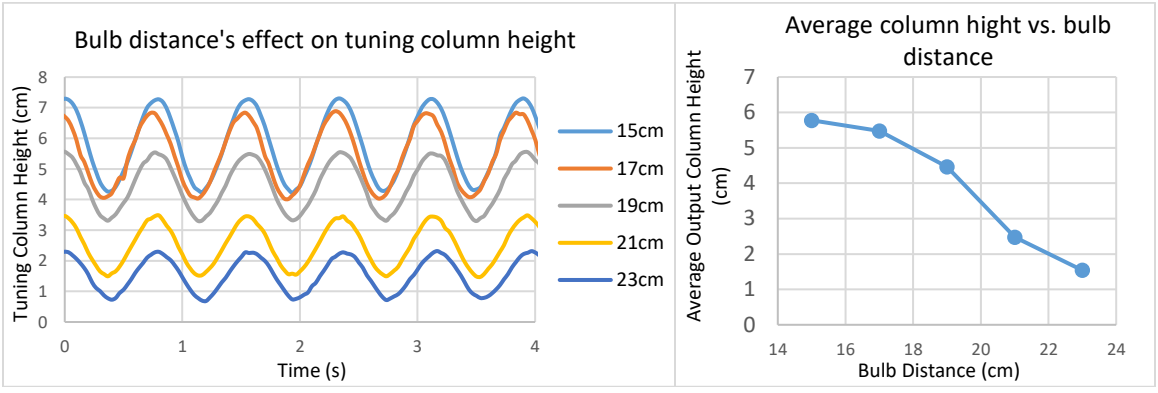

Figure 6.10: Radiative intensity's effect on solar engine performance
(A) Engine performance and (B) Average output column height with respect to bulb distance.
(C) Normalized engine performance and (D) amplitude of oscillation with respect to bulb distance.

There are several understandings that can be obtained from these results: Figure 6.8A, which shows the water level height in the output column, indicates that with increased intensity the gas chamber's average volume is larger than that of lower intensities. Figure 6.8C shows the output column oscillation distance normalized to the minimum distance of the cycle stroke. The results demonstrate that with the increased intensity, the amplitude of oscillation (thus output power) increases. There is nearly double the amplitude between the trials of the 15cm bulb distance as opposed to 23cm trail. Figure 6.8A and C both show that though internal volume and oscillation amplitude increase with increased input power, the frequency of oscillation remains unchanged. The results offer further merit to the understanding that engine geometry determines frequency of oscillation and input power determines amplitude and internal pressure[1], [12], [29].

6.2.3 Engine Scalability

A potential for deriving more useful power from the engines is increasing their size and thus stroke volume. If effective larger scaled engines could be built, more practical applications for water distribution and heat conversion could be realized. To test the scaling of size, two engines were created: one which increased the depth the other by the planar area. The depth scaled engine was constructed from the assembly of multiple 1/2", 1/4", and 1/8" acrylic panels bonded together to create a "3-Dimensional" engine (Dimensions found in Appendix D). This engine provided a six-fold increase to the depth in comparison to the planar engines, with the same column dimensions and area (Figure 6.11A). A second scaled engine, which was the largest engine created through the Sulchek lab, was a planar engine with area scaled by 1.5x that of a standard engine geometry used throughout this research (same geometry of the engine used in Chapter 4).

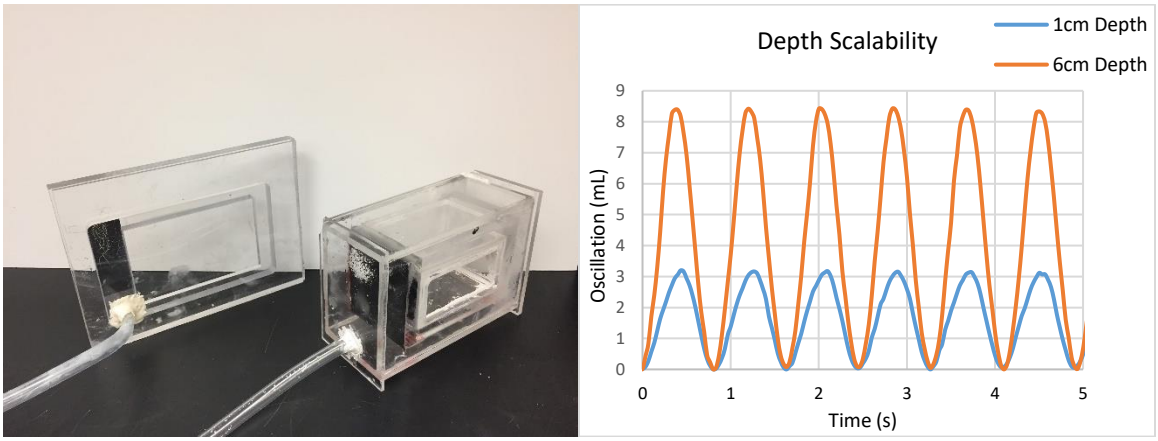

Figure 6.11: Solar engine scalability
(A) Engines used in depth scale testing (B) Performance of depth scaled engines
(C) Engines used in area scale testing (D) Performance of area scaled engines

The results from the depth scalability testing showed that a 2.8x increase in power output was achieved by a 6x increase in the engine depth. Note that frequency was unchanged by increasing engine depth which supports equation 5.4 stating that frequency is a function of column spacing and height.

The area scaling demonstrated interesting and unexpected results of a decrease in total power output with increase in area size, i.e. stroke volume was relatively unaffected, but frequency decreased with size. The results may be explained due to engines scaling by

area but *not depth*. To be truly scaled 1.5x in size the engine depth should have also been increased as well. Due to the fabrication process this was not done. By scaling area but not depth the surface area to volume ratio increased in the larger engine which likely contributed to poorer performance. Still the increase in surface area to volume ratio is likely not the only mitigating factor. The reduced relative performance is more likely due to decreased relative contribution of the vapor entry as discussed in chapter 5. Because the thermal entrance length (i.e. temperature differential) would be unchanged by scaling the engine area. Thus, the volumetric oscillation within the gas chamber would only be effected by height scaling. Additionally, any increase in amplitude do to vapor volume would likely be met with equal reduction from increase frictional drag. These factors may explain the zero net increase stroke volume.

7. Educational Outreach

Due to the simplicity of operation, the engine offers a unique potential as a learning aid to demonstrate principles of thermodynamics. Though limited in power output, the engine does possess a unique capability to demonstrate concepts of physics and thermodynamics in a clear, concise, and safe manner.

To address the need of learning aids to teach engine operation to students, we designed a kit consisting of the liquid piston engine, a range of liquids, and an educational packet which can be used in congruence with open source video processing software. The kit allows for students to get hands-on experience with a working engine and to visually see the cycle of expansion and compression of a chamber volume to produce mechanical work. The engines, which operate at a safe temperature range, are cheap to construct, and only require water and electricity to operate, make a perfect educational device to teach students principles of thermodynamics, engine cycles, heat transfer, and dynamics.

7.1 Thermodynamics Class Designette

The term designette was first coined out of the Singapore University of Technology and Design (SUTD) to describe short-term design charrettes [8], [10]. The designette is an example of active learning which requires a higher level of cognitive engagement than traditional lecturing. The designette aims to leverage the benefits associated with active learning and critical thinking required in the design process, in a short-term concise manner.

The designette technique was utilized for this first iteration of the liquid piston engines being used for student engagement. This designette was performed with for an undergraduate thermodynamics class at the Georgia Institute for Technology. For the

designette, groups of students could select from 12 unique types of engines and 3 different working fluids [8]. The engines ranged in 2 heights and 3 lengths with each geometry having/not having a steel wool regenerator. Also provided were 9V batteries to power the engines. The students were encouraged to creatively apply course material, their own knowledge of physics, and outside materials (i.e. ice baths, and multiple batteries) to achieve the highest efficiencies with their engines.

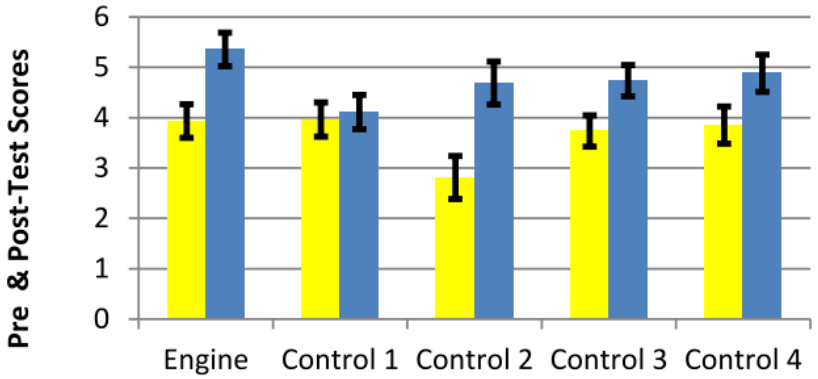

Figure 7.1: Pre & post-test results from thermodynamics designette [8]

To determine the effects the designette had on concept retention pre and post tests were used in comparison with 4 class section that did not participate in the designette. Though not found to be statistically significant, the group that participated in the engine designette did produce the highest post-test scoring.

The designette helped demonstrate the potential these engines have for providing a unique experience to the typical classroom experience.

7.2 High School Demonstrations

In the spirt of the short term designette, an interactive presentation has been developed to help encourage the understanding of how different variables may impact a

physical system. The demonstration shows how heat of vaporization, geometry, and input power may impact engine performance.

A class demonstration was performed with an AP physics class at Lassiter High School in Alpharetta GA. The demonstration was useful in collecting student feedback and teacher input on how to use these engines for education. The 55 minute class period was broken into 2 sections. The first section consisted of a 15 minute traditional power point presentation discussing fundamental concepts of physics, thermodynamics, and mass transfer by relating them to the engine. An emphasis was placed on how energy can manifest itself in many different forms. Because the engines deal with gas expansion, phase-change, and heat to mechanical work conversion, they serve as excellent tools to demonstrate potential and kinetic energy. The presentation also touched on feedback loops and hydraulic head which were new concepts for many of the students.

The second portion of the presentation included an interactive session where students applied some of the concepts discussed in the lecture and previously in their physics course. The students were broken up into 3 groups and were able to select from 3 engines demonstrating different attributes involving gas chamber volume. The students were also able to select from 3 different fluids to power their engine. Through competition the student groups were encouraged to achieve the greatest engine power output measured by volumetric oscillation. Due to limitations of the materials the students were restricted to selecting their 2 components in a draft like scenario where the first group to pick the engine was the last group to pick the fluid. This selection process encouraged students to think critical about the parameters which drive engine performance, weighing their options between working liquid and engine geometry. Along with the presentation, handouts were

given to the students which explained the activity and provided discussion questions (Appendix E)

Figure 7.2: Students actively learning

The demonstration was successful both in encouraging students to learn about heat to work conversion and actively apply knowledge learned in the presentation. Notably no group wanted to select an engine first as they determined liquid vaporization would be the primary driver in performance (this was a correct assertion). Additionally, none of the engines worked initially which encouraged students to question their initial set up and adjust fluid levels and engine tilt. All groups maximized power input, and were successful in collected data by the end of class.

The demonstration was successful in gaining valuable input on how the engine amd associated lab exercise can be improved for high school education. Through discussion with students and staff it has become clear that the engines would be most applicable to AP physics and Chemistry. Specifically, the lab developed around the engines may target the AP thermodynamics curriculum which discusses the laws of thermodynamics, briefly introduced thermodynamic cycles, and discuses phase change and heat of vaporization.

Additionally, AP physics may also utilize the engines as the course also discusses conservation of energy and the "kinetic theory of matter" which helps students understand the energy states of different phases of material.

The demonstration was also helpful in highlighting what is important for the lab to focus on and what is out of reach for students at the high school level. None of the students successfully completed the "Bonus Questions" of the questionnaire which asked low level fluid dynamics questions.

Start-up summer

A three member student team have formed a company with the Georgia Tech's start up summer program to explore the viability of these engines, and their corresponding manuals, as products used in schools. The goal of this start up is to create a concise and accessible laboratory experience for high school and undergraduate students.

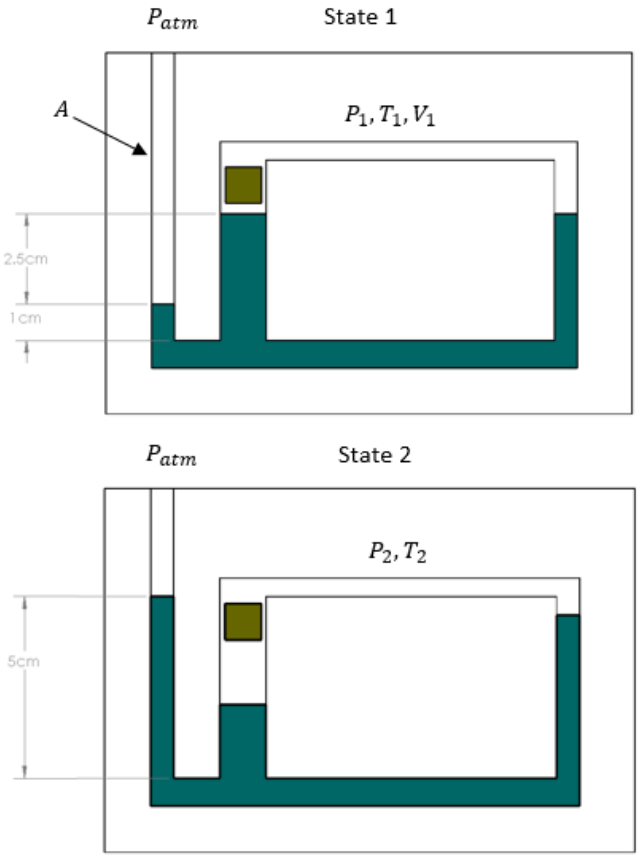

(a) What is the air chamber pressure (P_1) when the engine is at rest?

$$P_1 = P_{atm} - \rho g(.025)$$

(b) What is the air chamber pressure (P_2) when the output column reaches height of state 2?

$$P_2 = P_1 + \rho g(.04)$$

(c) Given V_1 What is the volume in the air chamber at state 2?

$$V_2 = A(.04) + V_1$$

(d) Given T_2, T_1, V_1 and assuming thermal equilibrium and dry air state 1, how much water (mol) has been vaporized to the air chamber at state 2? *Hint: Amagat's Law*

$$V_{air} = \frac{T_2 P_1 V_1}{P_2 T_1}$$

$$M_v = (V_2 - V_{air})/v_g$$

Figure 7.3: Sample questions from manual

Feedback from high school instructors suggest that there is in fact a market for these types of school kits. Companies such as Arbor Scientific and Carolina Biological sell small lab demonstration kits used by instructors. Competitive kits do exist but are limited in the field of thermodynamics. The kits are also often expensive or otherwise too rudimentary to affectively demonstrate the wide range of topics that may be discussed by the liquid piston engines.

$109 $109

Figure 7.4: Arbor Scientific thermodynamic lab kits
[33]

Additionally, the liquid piston engines offer a greater potential for quantitative data collection. With the ubiquity of smart phones, video recording and processing can be utilized for this collection.

The work performed through this lab has demonstrated that these kits do demonstrate a strong potential to fill a notable gap in existing products. Few competitive products exist that exhibit the same level for quantitative data collection and none combine so many concepts of physics and thermodynamics into one package.

8. Conclusion

The extensive work in studying this engine has led to several critical insights of the engine's operation and its potential future applications. These small engines offer a unique research opportunity to further explore the dynamics involved with thermofluidic oscillators. Additionally, they contain the potential to be useful at solving important problems in waste energy conversion.

8.1 Intellectual Content

Cycle analysis

Extensive data collection on the internal working conditions of the gas chamber, and the effects that vaporization of different working fluids have on performance, have led to agreeing conclusions on how vapor flow impact engine operation. It is clear that the vapor mass fluctuation of the working liquid to vapor is the driving mechanism behind these engines, and to optimize their performance involves using liquids with a low heat of vaporization relative to the supply temperature. This conclusion on working liquid selection is congruent with Markides group which researches two-phase thermofluidic oscillation with mechanical engines [3]. Though commonly referred to as liquid piston Stirling engines, this is a misnomer when referring to smaller, vapor driven engines.

Vapor entrance theory

The results from the geometry and scalability experiments demonstrate that there is an association between the length of the column spacing and the stroke volume achieved by oscillation. The vapor entrance theory provides a physical explanation for the empirical results of an optimal channel length found both in chapter 5 and 6. The theory also

demonstrates a unique combination of the enhancing and diminishing factors which creates the performance characteristics of the engine.

Flexible Engine

A completely novel invention, the flexible engine offers entry into realm of engineering that is little explored: derive heat conversion off dynamic and curved sources. There are multiple benefits associated with the use of PDMS: The engines resist higher temperatures than that of the acrylic engines, through use of molds the manufacturing can be scaled easily, and the engines can be molded together in sheets to create added coverage and increased output. This molding potential also creates the ability of make multiple columns and chambers providing more complex and targeted heat transfer points which could be used to cool flexible computer chips.

8.2 Future Directions

The contributions of works such as this have led to a better understanding of the operation of the liquid piston heat engine. There is still much to learn about the engine, its operation, and its potential applications. The following are some future directions this work can contribute towards, and areas where there is a potential for this system.

Up-THERM

The UP-Therm developed by Markides group in London has produced particularly promising results and demonstrates an effective use of the thermofluidic oscillation of a two-phase working fluid [3]. Two-phase thermofluidic oscillation, which is the primary driving force for our engine, is a relatively unexplored phenomenon that offers great potential. Through use of a single mechanical piston the system is able to operate in a much

more predictable manner than that of its fluid piston counterpart, thus allowing a more streamline approach to optimization.

Educational Products

Finally, the educational kits developed through the startup summer program offer strong immediately use for the acrylic liquid piston heat engine. With thermodynamics entering high school curriculums the engines offer a unique opportunity to give students hands on experience with engine cycles. There exists a need for these type of demonstration tools that can be integrated into a curriculum and encourage active learning. It is the hope that through this work that the engines may be used to increase student understanding of course material, as well as encourage more curiosity and research in the field of liquid piston engines.

8.3 Conclusion

The liquid piston engine demonstrates a unique operation not thoroughly understood in modern engineering. By further understanding and optimizing this cycle which operates on a two-phase oscillation of a working liquid: more powerful and efficient mechanisms can be created. By further exploring this field the simple, low maintenance, and easily manufactured engines could become an important part of how we manage water and waste energy.

APPENDIX A: LIQUID VAPORIZATION TEST ENGINE

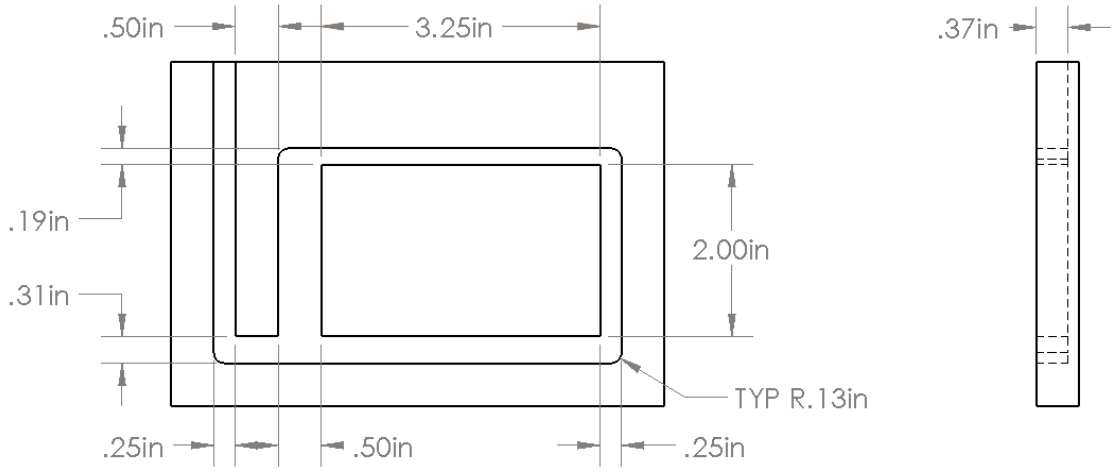

APPENDIX B: APPARATUS ENGINE

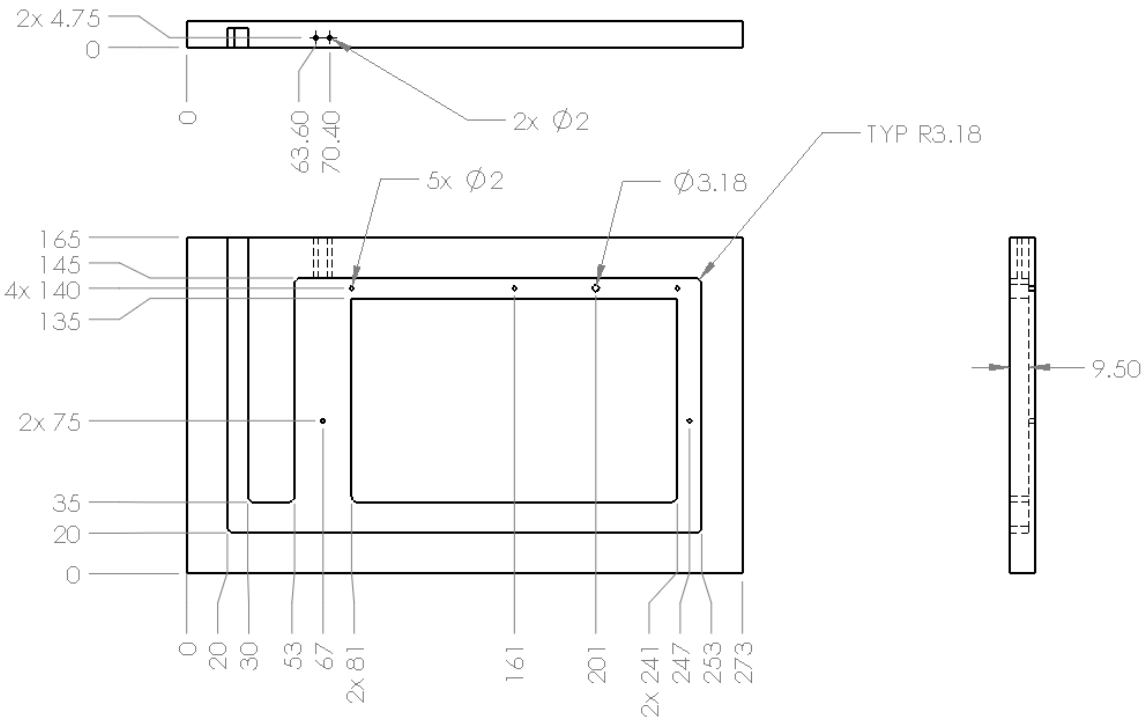

APPENDIX C: FLEXIBLE ENGINE

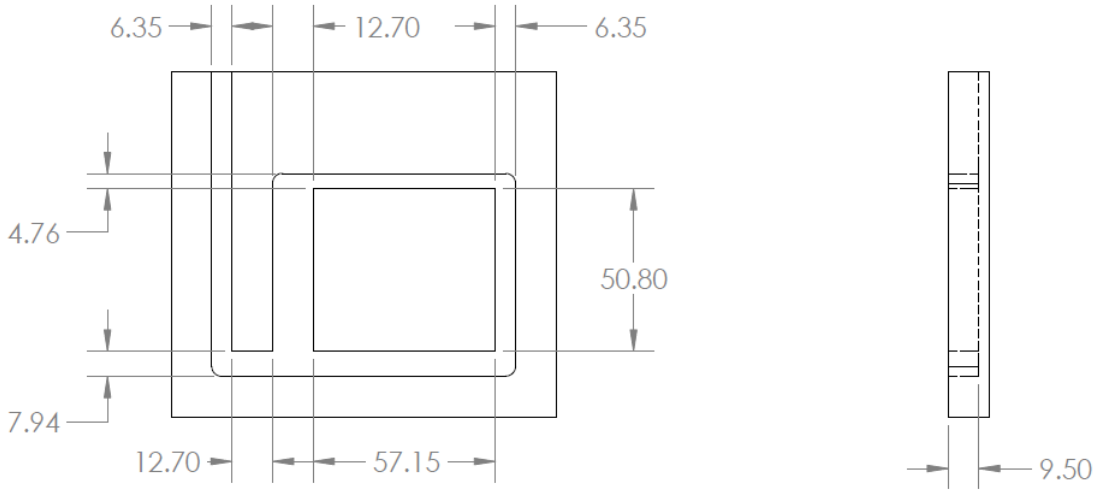

APPENDIX D: DEPTH SCALED ENGINE

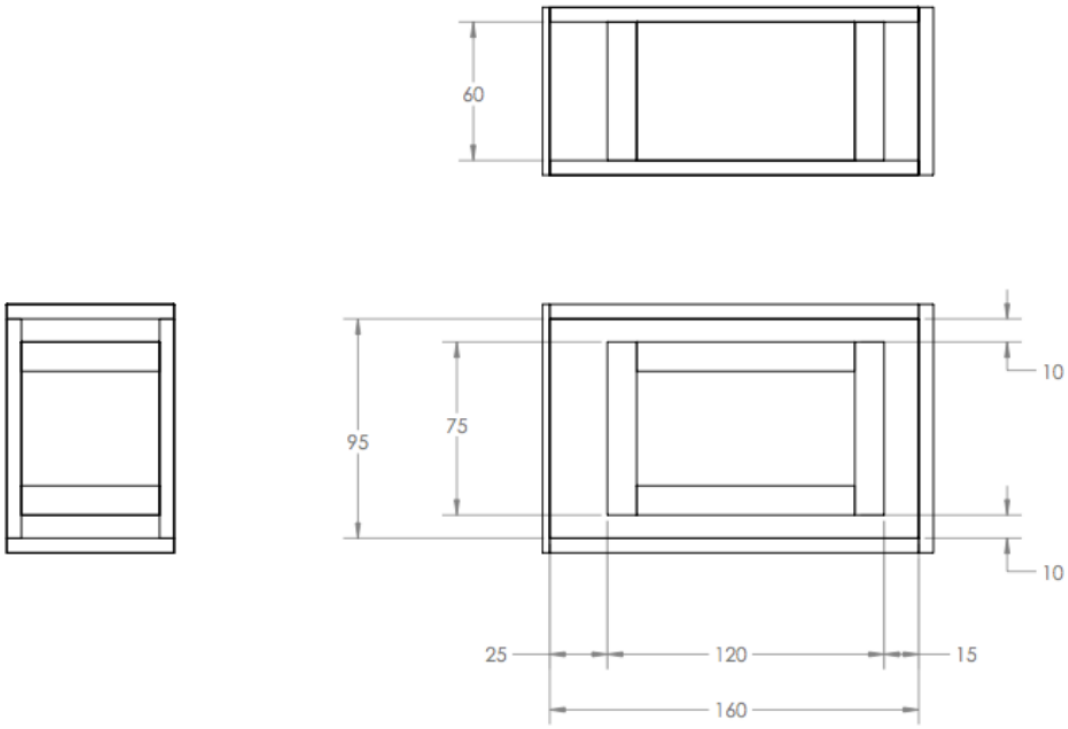

APPENDIX E: CLASS QUESTIONNAIRE

Questionnaire:

Engine #:_____

Fluid:_____

What was your reasoning for selecting this engine?

What was your reasoning for selecting this liquid?

What is the frequency of your engine?

To determine frequency: Recording the time it takes for 10 oscillations. Divide this time value by the number oscillations (10) to determine the period of one oscillation. Repeat this 3 times and take the average of the values. $f = 1/P$

What is your average peak-to-peak amplitude?

What is the input power of the engine?

What is the power output of the engine?

Use the Beale number equation: $W_o = B_n VPf$ where $B_n = 0.015$ and $V = Amplitude * Area$

Note: inner tube diameter = 7/16in

From question 3 and 4, what is the efficiency of the engine?

Discussion:

Assuming the ideal efficiency of the engine to be 1% list possible reasons for losses within the system.

In comparison to the efficiency of an internal combustion engine why is the efficiency of this engine low?

Discuss and explain steps you would undertake to reduce or eliminate these losses.

Explore and explain possible real world applications of the engine.

How could this demonstration be improved?

Bonus Questions:

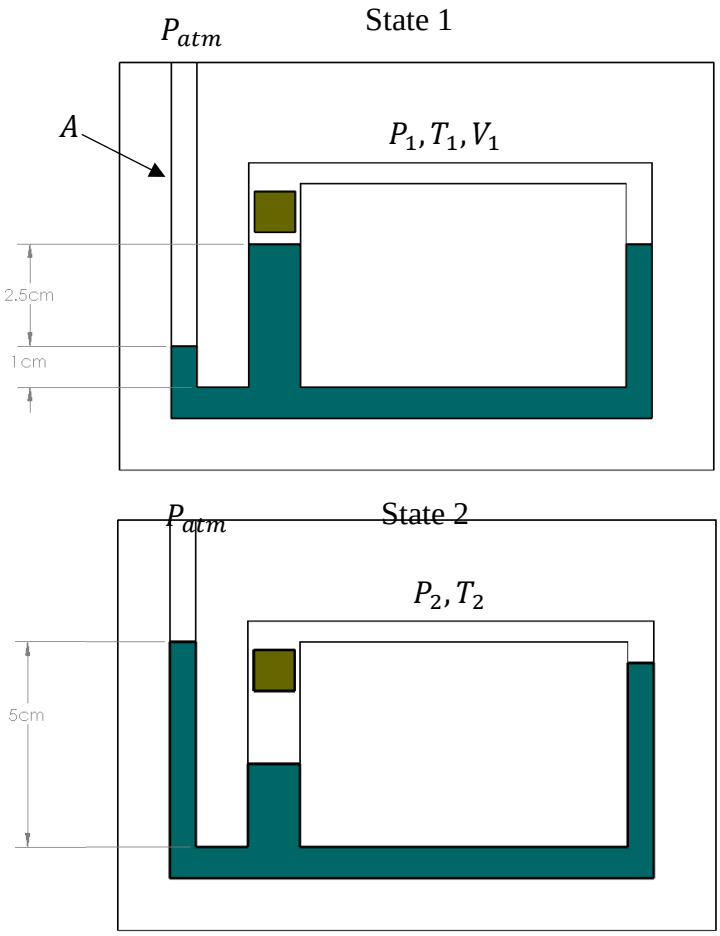

(a) What is the air chamber pressure (P_1) when the engine is at rest?

(b) What is the air chamber pressure (P_2) when the output column reaches height of state 2?

(c) Given V_1 What is the volume in the air chamber at state 2?

(d) Given T_2, T_1, V_1 and assuming thermal equilibrium and dry air state 1, how much water (mol) has been vaporized to the air chamber at state 2? *Hint: Amagat's Law (google it)*

Use terms:

Specific volume of vapor: v_g

Moles of water: M_w

Questions

REFERENCES

[1] N. Yang, R. Rickard, K. Pluckter, and T. Sulchek, "Integrated two-cylinder liquid piston Stirling engine," *Appl. Phys. Lett.*, vol. 105, no. 14, pp. 1–5, 2014.

[2] US Department of Energy, "Waste Heat Recovery - Technology and Opportunities in U.S. Industry," 2008.

[3] O. A. Oyewunmi, C. J. W. Kirmse, A. J. Haslam, E. A. Müller, and C. N. Markides, "Working-fluid selection and performance investigation of a two-phase single-reciprocating-piston heat-conversion engine," *Appl. Energy*, vol. 186, pp. 376–395, 2017.

[4] B. T. Liu, K. H. Chien, and C. C. Wang, "Effect of working fluids on organic Rankine cycle for waste heat recovery," *Energy*, vol. 29, no. 8, pp. 1207–1217, 2004.

[5] J. W. Stevens, "Low capital cost renewable energy conversion with liquid piston stirling engines," in *4th International Conference on Energy Sustainability*, 2010.

[6] S. K. Yee *et al.*, "$ per W metrics for thermoelectric power generation: beyond ZT," *Energy Environ. Sci.*, vol. 6, no. 9, pp. 2561–2571, 2013.

[7] E. Orda and K. Mahkamov, "Development of 'low-tech' solar thermal water pumps for use in developing countries," *J. Sol. Energy Eng. Trans. ASME*, vol. 126, no. 2, pp. 768–773, 2004.

[8] C. Telenko, S. K. Yee, J. S. Linsey, T. Sulchek, and W. C. Newstetter, "A Liquid Piston Engine Designette: Creative Learning in Thermodynamics," *4th Int. Conf. Des. Creat.*, no. 4th ICDC, pp. 1–8, 2016.

[9] B. A. Ross, "A simple Stirling engine for classroom use," in *of the 1981 IECEC*, 1981, pp. 1899–1902.

[10] C. Telenko *et al.*, "DESIGNETTES : AN APPROACH TO MULTIDISCIPLINARY ENGINEERING DESIGN Design and other fundamental topics in engineering are often isolated to dedicated courses . An opportunity exists to foster a culture of engineering design and multidisciplinary problem so," no. 2014, pp. 1–16.

[11] D. C. Mosby, "The Fluidyne Heat Engine," Naval Postgraduate School, 1978.

[12] C. D. West, *Liquid Piston Stirling Engines*. New York: Van Nostrand Reinhold Company Inc., 1983.

[13] N. Joshi, "A REVIEW ON STIRLING ENGINES," *Int. J. Innov. Res. Sci. Eng.*, vol. 2, pp. 221–226, 2016.

[14] A. Faghri, "Heat Pipes: Review, Opportunities and Challenges," *Front. Heat Pipes*, vol. 5, no. 1, 2014.

[15] R. Solanki, A. Galindo, and C. N. Markides, "Dynamic modelling of a two-phase thermofluidic oscillator for efficient low grade heat utilization: Effect of fluid inertia," *Appl. Energy*, vol. 89, no. 1, pp. 156–163, 2012.

[16] S. Backhaus and G. Swift, "A thermoacoustic Stirling heat engine," *Nature*, vol. 399, no. May, pp. 335–338, 1999.

[17] G. T. Reader, P. Ivett, G. Gill, and P. D. X. Lewis, "Modelling the jet-stream fluidyne," in *the 1981 IECEC*, 1981, vol. 2, pp. 1909–1915.

[18] T. C. B. Smith, "Asymmetric heat transfer in vapour cycle liquid-piston engines,"

in *12th International Stirling Engine Conference*, 2005, pp. 302–14.
[19] R. Fauvel, G. Walker, and G. T. Reader, "Excitation of a fluidyne tuning line," in *Proceedings of the 25th Intersociety Energy Conversion Engineering Conference IECEC-90*, 1990.
[20] M. Özdemir and A. F. Özgüç, "A simple mathematical model to analyse a fluidyne heat machine," *Proc. Inst. Mech. Eng. Part A J. Power Energy*, vol. 217, no. 1, pp. 91–100, 2003.
[21] L. Yu, R. Fauvel, Reader G, and G. Walker, "Application of the Fluidyne in Developing Countries," in *Intersociety Energy Conversion Engineering Conference*, 1992, pp. 411–415.
[22] J. W. Stevens, R. O. Kerns, and J. W. Mason, "Operational Characteristics of Liquid-Piston Heat Engines," *Whither Energy Conversion? Present Trends, Curr. Probl. Realis. Futur. Solut.*, pp. 1–12, 2014.
[23] J. D. Van de Ven, "Mobile hydraulic power supply: Liquid piston Stirling engine pump," *Renew. Energy*, vol. 34, no. 11, pp. 2317–2322, 2009.
[24] V. S. Slavin, G. C. Bakos, and K. A. Finnikov, "Conversion of thermal energy into electricity via a water pump operating in Stirling engine cycle," *Appl. Energy*, vol. 86, no. 7–8, pp. 1162–1169, 2009.
[25] C. R. Brunold, J. C. B. Hunns, M. R. Mackley ', and J. W. Thompson, "Experimental Observations on Flow Patterns and Energy Losses for Oscillatory Flow in Ducts Containing Sharp Edges," *Chem. Eng. Sci.*, vol. 44, no. 5, pp. 1227–1244, 1989.
[26] C. D. West, "Theoretical basis for the Beale Number," *Proc. 1981 IECEC*, vol. 2, pp. 1886–1887, 1981.
[27] D. Brown, "Tracker Video Analysis and Modeling Tool," 2017. [Online]. Available: http://physlets.org/tracker/.
[28] T. L. Bergman, A. S. Lavine, F. P. Incropera, and D. P. Dewitt, *Fundamentals of Heat and Mass Transfer*, 7th ed. Danvers, MA: John Wiley & Sons, Inc., 2011.
[29] C. W. Stammers, "The operation of the Fluidyne heat engine at low differential temperatures," *J. Sound Vib.*, vol. 63, no. 4, pp. 507–516, 1979.
[30] Y. A. Cengel and M. A. Boles, *Thermodynamics an Engineering Approach*, 7th ed. New York: McGraw Hill, 2011.
[31] W. Xu, N. Chahine, and T. Sulchek, "Extreme hardening of PDMS thin films due to high compressive strain and confined thickness," *Langmuir*, vol. 27, no. 13, pp. 8470–8477, 2011.
[32] J. E. Mark, *Polymer Data Handbook*. Oxford University Press, 1998.
[33] "Arbor Scientific, Tools that Teach," 2016. [Online]. Available: http://www.arborsci.com/. [Accessed: 27-Apr-2017].